J. Earth Syst. Sci. (2020)129 32
https://doi.org/10.1007/s12040-019-1296-1

Subduction–collision processes and crustal growth in eastern Dharwar Craton: Evidence from petrochemical studies of Hyderabad granites

Arijit Pahari[1], P Prasanth[2], Devleena M Tiwari[2], C Manikyamba[1,*] and K S V Subramanyam[1]

[1] *CSIR-National Geophysical Research Institute, Uppal Road, Hyderabad 500 007, India.*
[2] *Centre for Earth, Ocean and Atmospheric Sciences (CEOAS), University of Hyderabad, Hyderabad 500 046, India.*
**Corresponding author. e-mail: cmaningri@gmail.com*

MS received 12 April 2019; revised 6 September 2019; accepted 10 September 2019

The granite batholiths of eastern Dharwar Craton, which are showing intrusive relationship with TTGs, exposed in the eastern part of Telangana state at University of Hyderabad, Gachibowli (9.30 km^2), are studied for their petrographic and geochemical characteristics compared with their counterparts in EDC and evaluated their petrogenesis. These are predominantly microcline and quartz with subordinate plagioclase, exhibiting intergranular and perthitic textures. Geochemically, they are strongly peraluminous to slightly metaluminous in nature with high Alumina Saturation Index (ASI) ranging from 0.86 to 1.11 indicating the role of plagioclase in their genesis. Their alkali-calcic to alkalic nature, narrow range of Modified Alkali-Lime Index (MALI; Na_2O+K_2O-CaO), and low Fe-number reflect their similarities with the I-type Cordilleran granites. Prominent negative Europium anomalies, high Sr, Rb, Rb/Sr and low Sr/Y ratios indicate moderate to low pressure partial melting of pre-existing TTG with residual plagioclase in the source. We suggest, the melting of older TTGs through crustal anataxis process formed these granites and the sanukitoid melts supplied the required heat for the melting of TTG to evolve into granites. The genesis of these granites supports reworking of older crust, crustal differentiation during syn-collisional stage and marks the stabilization of continental crust in the Dharwar Craton during the Neoarchean time.

Keywords. Hyderabad granites; subduction–collision; crustal growth; Dharwar Craton.

1. Introduction

The formation of Archean continental crust and its secular changes with time and space provide significant constraints on the thermal and chemical evolution of mantle and its role in the evolution of various geodynamic processes through cooling and differentiation of mantle (Laurent *et al.* 2014; Jayananda *et al.* 2018; Singh *et al.* 2019). This mantle evolution took place through stagnant lid to plate tectonic processes among which few evidences of plate tectonics are preserved in the Meso-Neoarchean granite-greenstone terranes that are present in different cratons of the world. Granitic magmatism represents hydrous melting of mantle which is one of the evidences for the subduction zone magmatism uniquely observed on the planet Earth. According to Gastil (1960), the growth of continental crust recorded during 3.4, 3.0, 2.7, 1.7, 1.0 Ga, is present in all the cratons of

Published online: 20 December 2019

the world. However, majority of the researchers suggest that 2.7–2.5 Ga is a global peak in the growth of continental crust which is also evidenced from the Dharwar Craton, India (Taylor and McLennan 1985; Reymer and Schubert 1986; Condie 1989; Zhai 2014; Jayananda *et al.* 2019).

The Archean crustal corridor is comprised of three dominating litho types: (i) Tonalite–Trondhjemite–Granodiorite (TTG) which is mainly formed in the early phase; (ii) the volcano-sedimentary sequences of greenstone belts, and (iii) late stage anatectic high K granitic intrusion (Laurent *et al.* 2014). The late phase Archean granitic magmatism is very common in all the cratons of the globe which plays a pivotal role in the crust formation process, tectonic assembly, mineralization and stabilization of the cratons (Condie 1981, 2000; Martin 1993; Sylvester 1994; Moyen *et al.* 2003; Heilimo *et al.* 2011; Condie and Kröner 2013; Ram Mohan *et al.* 2013; Dey *et al.* 2012, 2014, 2017; Jayananda *et al.* 2018). It is widely believed that the Archean continental growth has been dominated by combined island arc and plume-related intra-plate magmatism (Naqvi and Rogers 1987; Fliedner and Klemperer 2000; Santosh *et al.* 2013).

The Dharwar Craton divulges the Paleo to Mesoarchean continental crust marked by a progressive transition from upper to lower crustal levels with basement-granite-greenstone terranes grading southward into granulites (Swami Nath and Ramakrishnan 1981; Janardhan *et al.* 1982; Radhakrishna 1983; Jayananda *et al.* 2013). Neoarchean granites and greenstone belts of EDC are encompassing most of the craton with a sparse remnant of >3.0 Ga TTG. The crust formation, its reworking and tectonomagmatic processes of EDC are explained through plume-arc accretion and cratonization (Manikyamba *et al.* 2004a, b, 2009; Smithies *et al.* 2009; Manikyamba and Kerrich 2012; Barnes and Van Kranendonk 2014). The granite batholiths of EDC are hosted by N–S trending shear zones, NNW–SSE greenstone belts (2.7 Ga), intruded by a variety of dykes (2.2–1.0 Ga) and became a stable craton with the emplacement of kimberlites at ∼900 Ma to 1.1 Ga (Rao *et al.* 2013). The vast granitic terrain of EDC exposed around Hyderabad (commonly known as the Hyderabad Granite batholith) is a combination of a variety of granitoids such as aplites, granites, granodiorites, monzogranites, syenogranites, alaskites, etc. (Praveen *et al.* 2018; Anjaneyulu *et al.* 2019). The Rb–Sr dates attest an age of 2500 Ma (Crawford 1969) and are correlated with the Closepet and Chitradurga granites of Dharwar Craton (Goutham *et al.* 2010). In general, the Hyderabad granites are mineralized with molybdenite at Pirancheru and Taramatipet (Saxena and Sudarshan 1997; Samal and Srivastava 2014). The molybdenite mineralization indicate their genesis in lit-par-lit injections of basaltic melts into the sialic crust. At places, the single pyroxene bearing granitoids, charnockite assemblages are reported from the Hyderabad granite batholith (Sitaramayya 1971; Madhusudhana Rao *et al.* 2002). The genesis of granitic batholiths (huge granitic exposures) like Sierra Nevada (North America), California (North America), South Mountain (Nova Scotia), Patagonian (Chile), Cordillera-Blanca (Peru), New England (Australia) batholiths are highly debatable in terms of melt accumulation, source, hybridization, metasomatism (potash–boron) and tectonic emplacement. In the geological history, 2.5 Ga is marked as the granitic boom covering the entire world and the Indian cratons are not exempted from this process. Further, this granitization event is linked with the onset of plate tectonics, crustal reworking and growth of supercontinents. The lower crustal remelting of thick older TTG gneisses is responsible for the growth of granitic batholiths through assimilation and fractional crystallization, which are the dominant magmatic processes for which the basaltic magmatism acted as a heat source (Huppert and Sparks 1988). Hyderabad granite batholith is a composite granitic body exhibiting a variety of granitoids that are exposed at different places in Telangana and Andhra Pradesh displaying variable petrological, geochemical characteristics and mineralization. Present study deals with the geochemical characteristics of granites from the eastern part of eastern Dharwar Craton to understand the genesis and their role in the crustal evolution processes. This work unravels the late phase granitic intrusion in the EDC which is a significant contribution in the advent of Neoarchean crustal accretion and geodynamic setting. Through geochemical signatures, we evaluate the role of ancient crust (Mesoarchean) in the genesis of the studied Hyderabad granites, which provide insights into the tectono-magmatic processes and its implications on the Neoarchean–Paleoproterozoic crustal growth in the eastern Dharwar Craton.

2. Regional geology

Dharwar craton is one of the oldest cratons in the southern peninsular India, ranging in age from 3.4 to 2.5 Ga, recorded the Paleo to Neoarchean

magmatic events which are related to crust formation and its reworking that have significantly contributed in the evolution of continental crust (Peucat *et al.* 1995; Balakrishnan *et al.* 1999; Chadwick *et al.* 2000; Jayananda *et al.* 2000, 2006, 2008, 2018; Ramakrishnan and Vaidyanadhan 2010; Manikyamba *et al.* 2017; Pahari *et al.* 2019). The Dharwar Craton is best known for the development of extensive greenstone sequences, grey gneisses and younger granites (Ramakrishnan and Vaidyanadhan 2010). It has been subdivided into western (WDC) and eastern Dharwar craton (EDC) on the basis of the nature of greenstone belts, grade of metamorphism, degree of melting, crustal thickness and tectono-magmatic evolution (Naqvi and Rogers 1987; Jayananda *et al.* 2000; Moyen *et al.* 2003; Ramakrishnan and Vaidyanadhan 2010). The combined geophysical, geochemical and structural studies suggest that the evolution of WDC initiated ∼3.4 Ga that is recorded in the peninsular gneisses (Guitreau *et al.* 2017) which is stratigraphically overlained by the Dharwar supergroup consisting of komatiites-basalt association with various types of clastic and chemical sediments and late stage dykes. The Neoarchean greenstone belts of EDC are associated with 2.7 Ga gneisses (TTG), transitional TTGs, high Mg granitoids and 2.5 Ga younger potassic anatectic granites with sporadic occurrence of the older peninsular gneisses (Balakrishnan *et al.* 1990, 1999; Krogstad *et al.* 1991; Peucat *et al.* 1993; Jayananda *et al.* 1995, 2000; Chadwick *et al.* 2000; Sarvothaman 2001; Moyen *et al.* 2001, 2003; Chardon and Jayananda 2008; Dey *et al.* 2014; Nandy *et al.* 2019). Jayananda *et al.* (2019) reported zircon U–Pb ages, Nd isotopes, major and trace element data for the magmatic-epidote bearing granitic plutons from Bellur–Nagamangala–Pandavpura corridor of WDC, suggested three successive episodes of anataxis, crustal reworking and continent generation in the WDC at 3.2, 3.0 and 2.6 Ga. Dey *et al.* (2017) reported Secondary Ion Mass Spectrometer (SIMS) U–Pb zircon dates on the granitoids of the NW part of the EDC to understand their origin and sequence of emplacement in EDC. The granitoid magmatism in the northwestern part of the eastern Dharwar Craton (EDC), initiated at 2.68 Ga with gneissic granodiorites of intermediate composition between sanukitoid and TTG. This was followed by intrusion of transitional TTGs (large-ion lithophile element-enriched) at 2.58 Ga. The sanukitoid to Closepet type magmatism with the intrusion of K-rich leucogranites mark the cratonization at 2.53–2.52 Ga. Dey *et al.* (2017) suggested that micro plates were the possible source of older crustal signatures and their accretion appears to be one of the important processes of Neoarchean crustal growth globally. Li *et al.* (2018) documented multiple subduction and amalgamation of several microblocks in the Dharwar Craton and its southern domains during the Archean–Paleoproterozoic transition. Their geochemical data suggest low degree partial melting of a metasomatized peridotitic mantle wedge with reworking of older continental crust. Based on bulk rock geochemical data on the banded gneisses, TTG, biotite granites, alkali feldspar granite and gabbro associated with the metabasalts of Neoarchean Tsundupalle greenstone belt, Nandy *et al.* (2019) identified diverse sources, including both crust and enriched mantle in an evolving subduction zone. A convergent orogenic setting is proposed for interpreting the association of various granitoids in the Tsundupalle area. The porphyritic granitoids of Adoni area which are intrusive into the Peninsular Gneissic Complex (PGC) of eastern Dharwar Craton are suggested to have been generated from low pressure-high temperature partial melting of a tonalitic–granodioritic crust (Singh *et al.* 2017). The geochemical characteristics of the Neoarchean granites and associated mafic microgranular enclaves (MMEs) from the Nalgonda region, EDC, indicate the magma mixing processes in the genesis of the host granite with differences in the degree of dilution of mafic magma and diffusive fractionation processes in a subduction zone environment (Jayananda *et al.* 2014; Shukla and Ram Mohan 2019). Narasimha *et al.* (2018) studied the whole rock geochemical characteristics of the Punugodu granites of Nellore schist belt, eastern Dharwar Craton and interpreted them as within plate anorogenic A-type granites.

The granites from Hyderabad region are confined to Precambrian younger gneissic complex in the northeastern part of eastern Dharwar Craton covering Karimnagar–Mahaboobnagar–Warangal districts, bounded by Karimnagar granulite belt and Godavari Graben in the northeast, Proterozoic Cuddapah basin in the south and Deccan Traps in the northwest (figure 1). The Gadwal, Peddavuru, Ghanapur, Yerraballi greenstone belts and sedimentary rocks of Mulugu sub-basin of Pakhal Supergroup are located alongside of the Hyderabad batholith. This composite batholith has discrete root extending to a depth of more than 10 km,

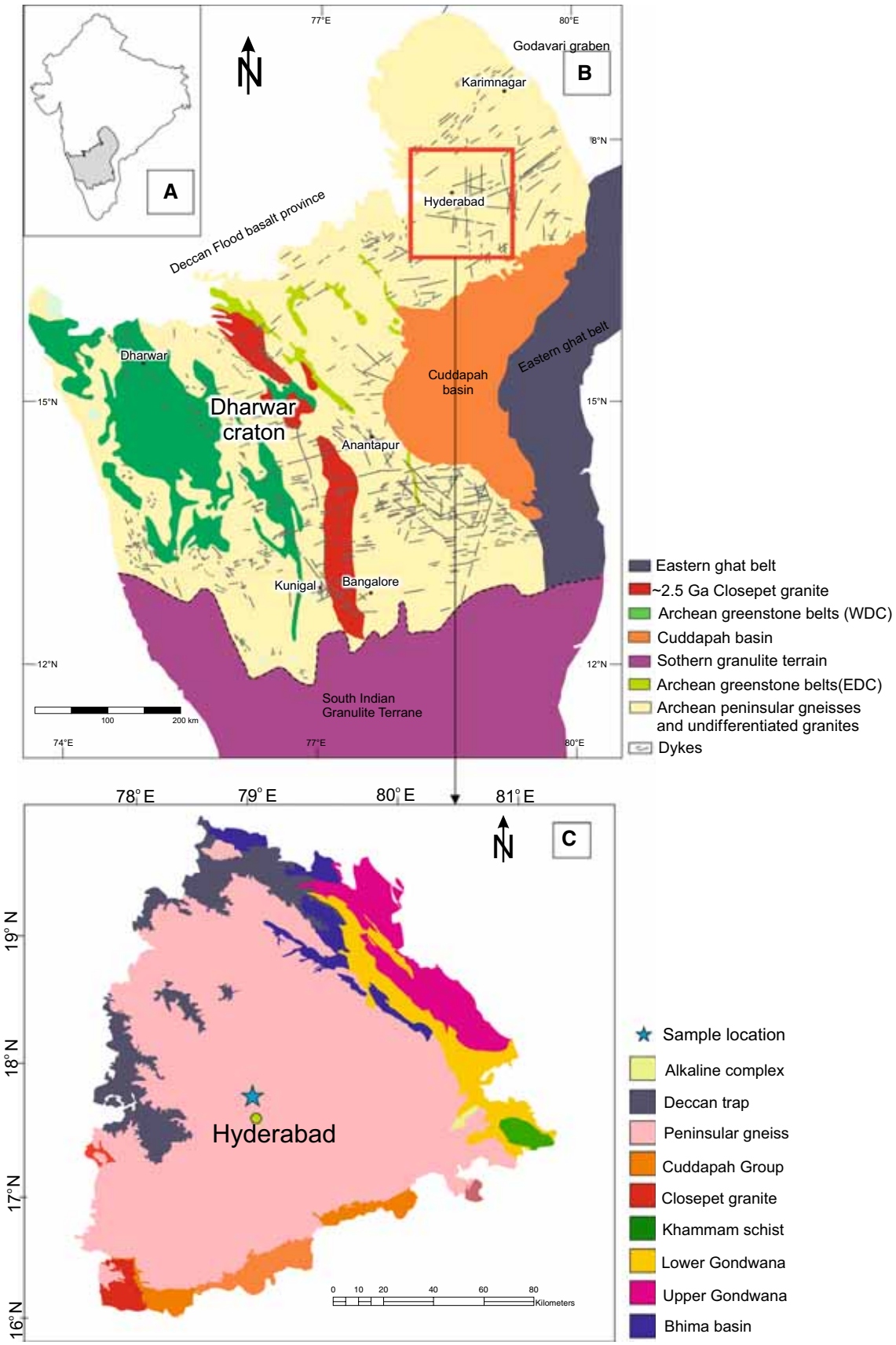

Figure 1. (**a**) Inset map showing Dharwar Craton in southern India. **(b)** Detailed geological map of Dharwar Craton (modified after French and Heaman 2010) and **(c)** geological map of Telangana state showing the study area and sample location (after GSI 1995; Shukla and Ram Mohan 2019).

covering an area of 10000 km^2, consisting of several criss-cross major and minor lineaments, pre-existing faults which are responsible for vertical adjustments and Neotectonic activity (Pandey *et al.* 2002; Singh *et al.* 2004). ENE–WSW and NNW–SSE mafic dykes are widespread throughout this batholith (Murthy 1995; Radhakrishna *et al.* 2004).

3. Sampling and analytical techniques

The study area is situated in the eastern part of Telangana state, bounded by 17.461275–17.450945°N and 78.334359–78.311964°E, respectively (figure 1), covering an area of ∼9.3 km^2. Samples for the present study were collected in and around the University of Hyderabad region from fresh outcrops which are devoid of siliceous and carbonate veins (figure 2). The studied granites are grey to slight pink in colour, leuco to slightly melanocratic, and characterized by coarse to fine grained equigranular K-feldspar, plagioclase and quartz as essential minerals and biotite occurring as accessory mineral (figure 2a). Porphyritic varieties also are found with phenocrysts of potash feldspar (2–3 cm) present within the groundmass of quartz, microcline and plagioclase feldspar (figure 2b). At some places, occurrence of mafic minerals (biotite) within the felsic groundmass are observed with some patchy occurrence in between the felsic counterpart (figure 2c, d). These granites are massive and undeformed in nature except few outcrops in which the biotites are showing a linear banding due to local shearing.

After petrographic screening for alteration, 11 samples were selected for geochemical studies (table 1). Samples were crushed and powdered using agate mill and pulveriser (200 mesh) respectively. Pressed pellets were used to determine the major element concentrations on the X-Ray Fluorescence Spectrometer (XRF; Phillips MagicPRO 1400) at CSIR-National Geophysical Research Institute (CSIR-NGRI) with a relative standard deviation of 3% and the analytical procedure is referred to Krishna *et al.* (2007). For trace element analysis, the samples were dissolved following the closed digestion procedure. 50 mg representative sample powders were dissolved in savillex® vessels containing 10 ml acid mixture of HF: HNO_3 in 7:3 proportion, and kept on hot plate at 150°C for 48 hours. After complete digestion, 2–3 drops of perchloric acid ($HClO_4$) was added and the entire mixture was evaporated to complete dryness. Freshly prepared 20 ml of 1:1 HNO_3 was mixed and kept on hot plate at ∼80°C for 10–15 min. After obtaining clear solution, 5 ml of Rh (1 ppm concentration) was added as an internal standard and made into 250 ml. 5 ml of this solution was further diluted to 50 ml to

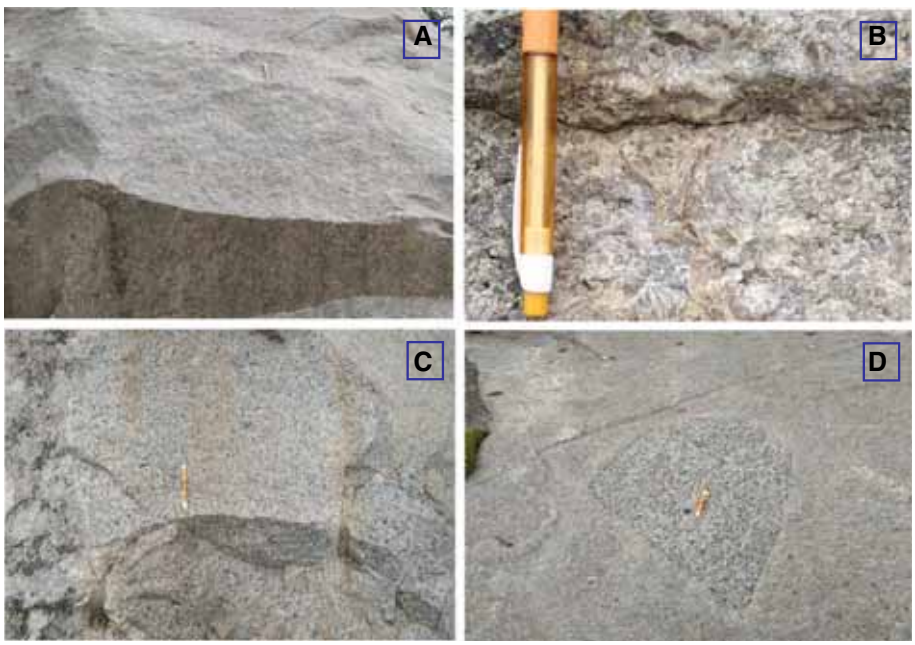

Figure 2. Field photographs of **(a)** granitic batholith, **(b)** potash feldspar phenocrysts within the granite, **(c)** concentration of mafic minerals (biotite) within felsic portion consisting of quartz and alkali feldspar, and **(d)** patchy appearance of mafic minerals in the outcrop scale.

Table 1. *Major, trace and rare earth element composition of granites from Hyderabad (EDC).*

Sample	SQ-1	SQ-2	SQ-3	SQ-4	SQ-5	SQ-6	SQ-7	SQ-8	PB1	PB2	MR1
wt.%											
SiO_2	72.38	68.04	72.20	73.14	72.22	76.83	70.19	71.60	73.58	72.24	72.45
TiO_2	0.30	0.33	0.20	0.24	0.32	0.16	0.36	0.14	0.28	0.18	0.26
Al_2O_3	14.18	14.79	14.29	14.14	14.83	12.37	14.91	14.33	13.68	14.49	13.66
Fe_2O_3	2.70	2.68	1.75	1.91	2.96	1.32	2.72	1.40	2.03	1.83	2.33
MnO	0.01	0.06	0.03	0.03	0.03	0.02	0.04	0.02	0.03	0.03	0.03
MgO	0.45	0.67	0.26	0.43	0.51	0.16	0.64	0.33	0.40	0.31	0.38
CaO	1.31	2.64	1.19	1.13	0.84	1.33	1.30	1.18	1.29	1.00	1.33
Na_2O	3.33	3.11	3.40	3.37	2.12	2.89	3.22	4.17	3.39	3.54	3.06
K_2O	4.90	4.55	5.24	5.05	5.98	4.48	5.57	5.88	4.85	5.18	4.97
P_2O_5	0.12	0.10	0.08	0.09	0.10	0.06	0.19	0.05	0.15	0.08	0.14
LOI	1.08	1.18	0.80	1.20	0.90	1.01	1.10	0.90	0.90	0.80	0.90
Total	100.78	99.16	99.43	100.72	100.81	100.72	100.23	100.00	100.57	99.68	99.50
MALI	6.92	5.02	7.45	7.29	7.26	6.04	7.49	8.87	6.95	7.72	6.7
FeO	2.43	2.41	1.57	1.72	2.66	1.19	2.45	1.26	1.83	1.65	2.10
Na_2O+K_2O	8.23	7.66	8.64	8.42	8.10	7.37	8.79	10.05	8.24	8.72	8.03
ASI	1.02	0.99	0.99	1.01	1.11	0.97	1.01	0.86	0.98	1.01	1.00
K_2O/Na_2O	1.47	1.46	1.54	1.50	2.82	1.55	1.73	1.41	1.43	1.46	1.62
ppm											
Cr	130	162	146	148	132	157	110	91	146	142	134
Co	4.12	10.42	3.44	3.58	4.55	2.54	4.50	3.05	3.60	2.97	3.84
Ni	7.10	8.61	14.60	8.62	8.40	9.26	13.40	9.03	15.96	7.60	8.61
Rb	313	278	329	297	350	257	334	313	284	369	285
Sr	145	235	167	155	91	222	164	198	133	123	172
Cs	1.46	3.15	1.49	0.71	0.64	1.21	1.15	0.76	0.83	0.91	1.51
Ba	476	466	489	459	487	474	531	471	472	469	572
Sc	3.46	9.06	2.40	3.11	4.78	1.95	3.78	1.95	5.57	2.85	2.98
V	28	61	20	21	36	27	29	22	24	19	27
Ta	1.93	0.69	1.61	2.12	1.53	1.18	2.52	1.40	5.50	2.55	1.74
Nb	23.87	16.04	17.83	24.04	27.78	12.50	30.14	10.28	41.86	21.42	21.07
Zr	467	397	424	498	408	261	690	325	358	319	464
Hf	11.77	10.41	11.12	12.69	10.98	6.84	17.25	8.59	10.26	8.58	11.56
Th	99	43	84	108	133	50	133	76	61	58	86
U	15.98	10.77	24.74	30.43	38.29	10.60	52.84	10.66	25.14	14.20	21.11
Y	35.67	23.49	26.36	30.28	31.05	17.65	39.05	20.42	44.30	24.04	26.07
La	120.55	17.79	96.69	120.95	245.60	63.70	147.09	69.63	72.95	57.73	115.79
Ce	216.86	39.14	169.68	201.90	382.56	112.54	259.87	114.97	142.12	99.39	191.85
Pr	25.53	6.31	19.68	22.48	37.73	13.21	30.04	13.77	18.65	11.68	21.33
Nd	73.71	23.51	55.60	61.46	91.85	37.56	84.03	40.31	57.73	34.04	57.74
Sm	12.22	5.71	8.95	9.68	11.01	6.27	13.48	7.54	10.96	5.83	8.78
Eu	1.26	0.93	1.02	1.17	1.42	0.72	1.48	0.99	1.28	0.87	1.17
Gd	7.25	3.86	5.22	5.79	6.13	3.65	7.91	4.66	6.78	3.74	5.10
Tb	1.22	0.71	0.88	0.98	0.91	0.62	1.33	0.80	1.24	0.65	0.85
Dy	5.51	3.34	3.95	4.43	4.09	2.74	6.01	3.59	5.91	3.13	3.91
Ho	0.91	0.58	0.66	0.75	0.72	0.46	0.99	0.57	1.04	0.56	0.64
Er	2.65	1.76	2.02	2.23	2.30	1.35	2.90	1.57	3.32	1.77	1.93
Tm	0.41	0.28	0.32	0.36	0.39	0.22	0.45	0.24	0.56	0.30	0.31
Yb	2.75	1.95	2.14	2.43	2.80	1.42	3.10	1.52	3.97	2.11	2.17
Lu	0.42	0.33	0.34	0.38	0.46	0.23	0.49	0.23	0.61	0.34	0.36
Cu	1.46	1.41	1.51	1.47	1.44	1.33	1.71	1.48	1.47	1.37	1.46
Pb	48	34	65	53	76	63	93	52	47	52	62
Zn	106	28	140	63	93	162	167	88	59	64	64
Ga	21	17	20	21	23	13	21	16	19	19	19
Total REE	471.25	106.20	367.14	434.99	787.97	244.68	559.19	260.38	327.10	222.15	411.94

Table 1. *(Continued.)*

Sample	SQ-1	SQ-2	SQ-3	SQ-4	SQ-5	SQ-6	SQ-7	SQ-8	PB1	PB2	MR1
Eu/Eu*	0.41	0.53	0.46	0.48	0.53	0.46	0.44	0.51	0.45	0.57	0.53
$(Th/Nb)_N$	34.79	22.31	39.55	37.70	40.09	33.52	36.99	61.78	12.23	22.54	34.09
$(Ce/Pb)_N$	0.38	0.35	0.22	0.32	0.43	0.15	0.24	0.19	0.25	0.16	0.26
$(La/Nb)_N$	5.24	5.81	5.63	5.22	9.18	5.29	5.06	7.03	1.81	2.80	5.70
$(La/Yb)_N$	29.82	33.86	30.72	33.87	59.52	30.55	32.24	31.02	12.48	18.57	36.24
$(La/Sm)_N$	6.16	8.20	6.75	7.80	13.93	6.35	6.82	5.77	4.16	6.18	8.23
$(Gd/Yb)_N$	2.13	1.60	1.98	1.93	1.77	2.09	2.07	2.47	1.38	1.43	1.90

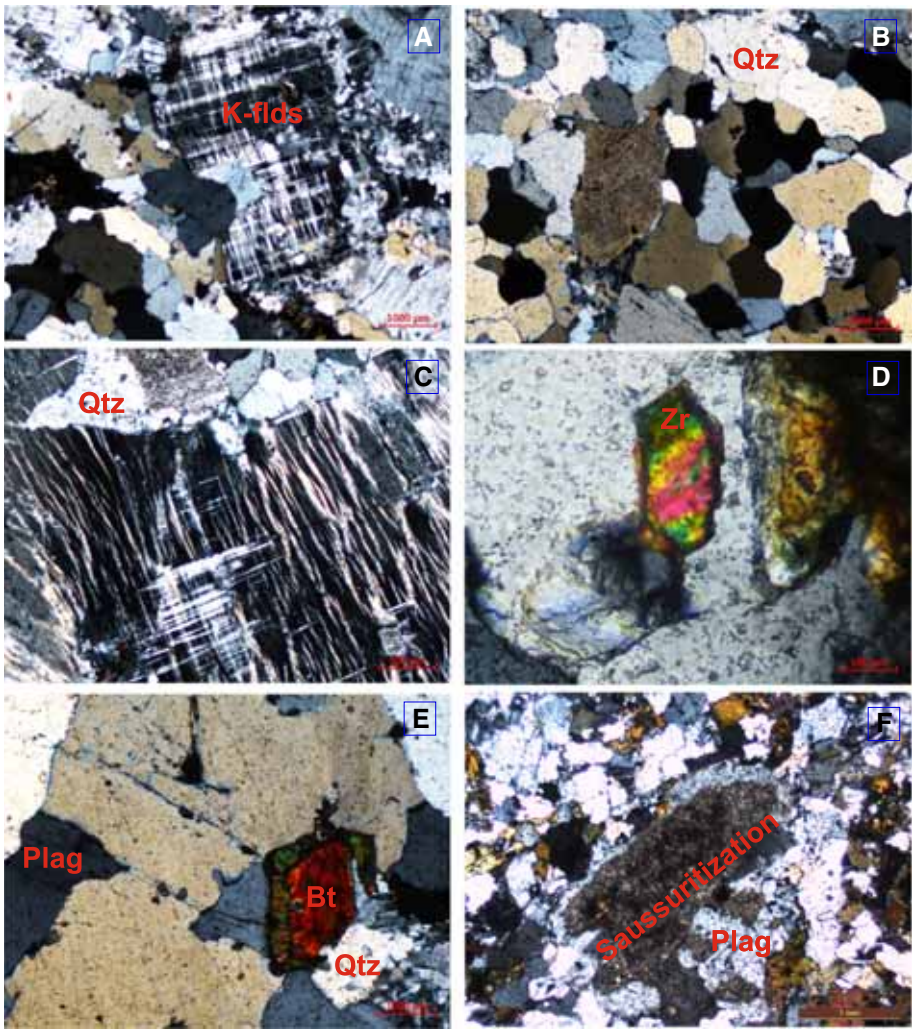

Figure 3. (**a**) Microcline occurring between the interstitial spaces of anhedral quartz and plagioclase displaying intergranular texture, **(b)** interlocking texture in quartz grains with occurrence of alkali feldspar in the interstitial spaces, **(c)** 'string variety' perthitic texture showing well developed plagioclase feldspar (albite) lamellae in K-feldspar host, **(d)** Euhedral zircons present in some sections, **(e)** parallel alignment of biotite due to local shearing, and **(f)** saussuritization observed in few sections due to the alteration of plagioclase feldspar.

achieve suitable TDS (total dissolved solids). Certified reference materials of Geological Survey of Japan (JG-2 and JG-1a) were run as standards during the analysis of major and trace elements. Precision and reproducibility obtained for international reference materials are found to be <5% RSD for the majority of the trace elements (Manikyamba *et al.* 2016).

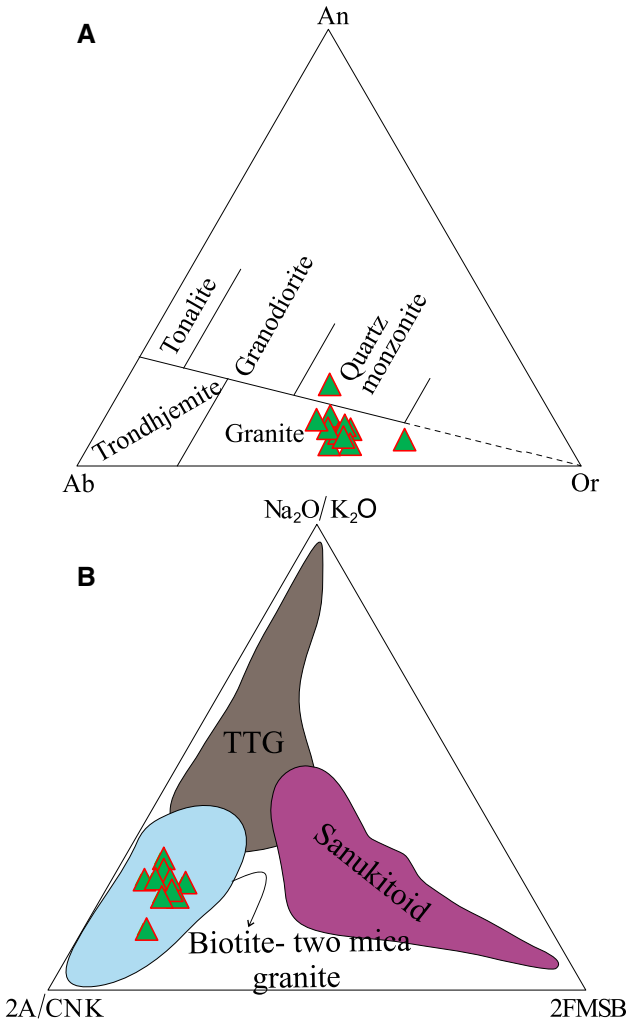

Figure 4. (**a**) Ternary diagram An–Ab–Or displaying granite field for the studied sample (after O'Connor 1965), **(b)** on Ternary diagram ($(Na_2O/K_2O)-2*A/CNK$ (molar $Al_2O_3/[CaO+Na_2O+K_2O]$)–$2*[(FeO_t+MgO)$ wt.% $*(Sr+Ba)$wt.%] =FMSB)) of Laurent *et al.* 2014) the granites are occupying the biotite-two mica granite field.

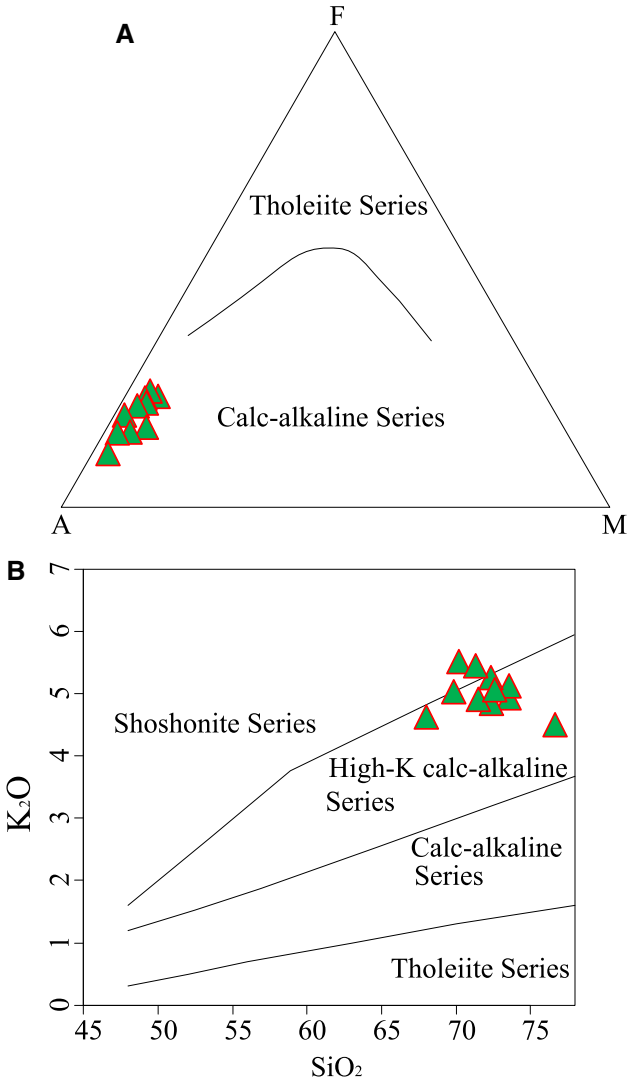

Figure 5. (**a**) AFM diagram (Irvine and Baragar 1971) indicating the calc-alkaline trend for these studied granites, **(b)** SiO_2 vs. K_2O relationship in which granites straddle high K-calc-alkaline to slightly shoshonitic field (after Peccerillo and Taylor 1976).

4. Petrography

The studied granites are homogeneous and devoid of magmatic banding in plane polarized light. They display a consistent modal composition with microcline (∼45%), plagioclase feldspar (An_{16-32}∼15%), quartz (∼35%) and biotite (∼5%). The accessory minerals are tourmaline, zircon, apatite, titanite and magnetite. The granites are coarse grained, inequigranular with subhedral microcline, anhedral quartz and plagioclase. The microcline occurs between the interstitial spaces of anhedral quartz and plagioclase displaying intergranular texture (figure 3a). Interlocking texture for quartz grains is observed in some samples and quartz is showing its typical wavy extinction and predominantly occurring in interstitial spaces of alkali feldspar (figure 3b). Perthitic texture is observed in most of the samples which are mainly 'string variety' showing well developed plagioclase feldspar (albite) lamellae in K-feldspar host (figure 3c) and euhedral zircons are present in few samples (figure 3d). In some sections, biotites, with typical bird's eye extinction display parallel alignment which is a signature of local shearing (figure 3e). At places, the cumulophyric, hypidiomorphic and porphyritic textures are also observed. Quartz and alkali feldspar are showing granophyric texture where they penetrate each other as feathery irregular intergrowth. Rarely, saussuritization is observed in some sections (figure 3f).

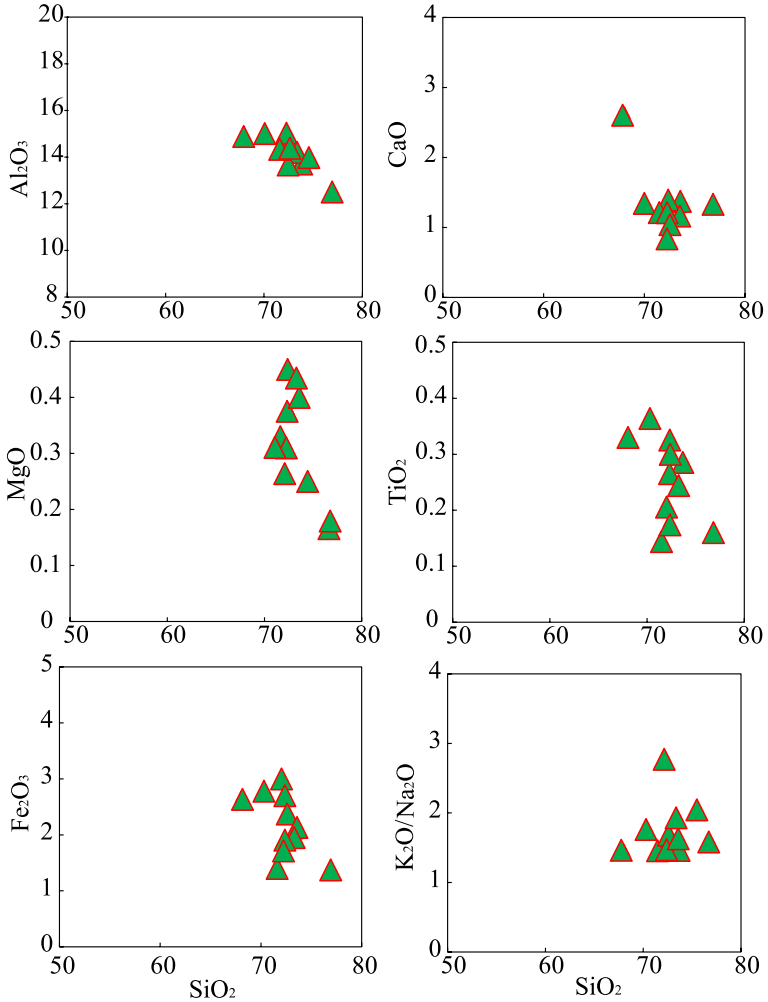

Figure 6. SiO_2 vs. major elements relationship exhibiting magmatic trends for these granites.

5. Geochemistry

The studied granites have high silica content (68.04–76.83 wt.%), moderate CaO (0.84–2.64 wt.%) and low MnO, MgO and TiO_2. The granites are characterized by high total alkalies (7.66–10.05 wt.%) and moderate to high aluminium content (12.37–14.83 wt.%). The K_2O concentration in these granites range from 7.66–10.05 wt.%, while the Na_2O is between 2.12 and 4.17 wt.% and the high K_2O/Na_2O ratio reflect on predominance of K-feldspars which is also supported by higher modal abundance of microcline. The ternary relationship between Ab–Or–An effectively classify the granitoids based on varied proportions of minerals present in solid solution series in which the studied samples predominantly occupy the granite field (O'connor 1965; figure 4a). Further, sanukitoids, two mica granites and TTGs can be effectively classified based on major element chemistry. On Na_2O/K_2O–2A/CNK–2FMSB ternary relationship, the studied samples plot in the biotite-two mica granite field with high A/CNK ratio reflecting on the hydrous and potassic nature of these granitic melts (Laurent *et al.* 2014; figure 4b). On AFM diagram, these granites are showing calc-alkaline trend reflecting on typical arc signatures (Irvine and Baragar 1971; figure 5a). High K calc-alkaline to shoshonitic characteristics are corroborated based on the relationship between SiO_2 and K_2O, which is also evidenced by the abundance of microcline in these granites (Peccerillo and Taylor 1976; figure 5b). Negative correlation between Al_2O_3, CaO, MgO, TiO_2, Fe_2O_3 and positive trend with K_2O/Na_2O with respect to SiO_2 is observed in these rocks (figure 6). Among the trace elements, Rb/Sr, Sr, Nb and Ba are displaying negative correlation with the increase of SiO_2 (figure 7). The studied granites are exhibiting higher abundance of large ion lithophile elements (LILE) such as Rb, Sr,

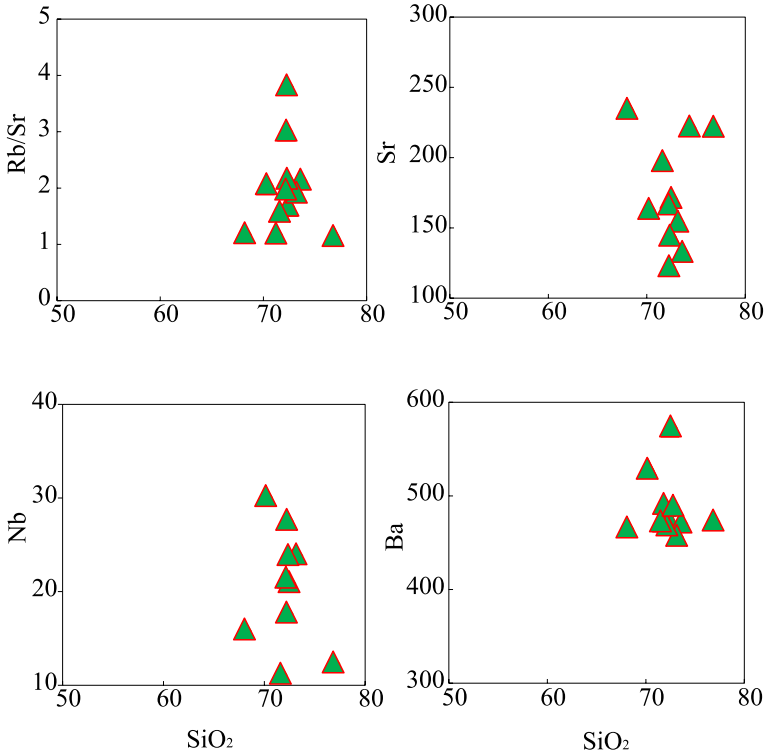

Figure 7. SiO_2 vs. LILE and HFSE relationship exhibiting negative correlation for the studied granite.

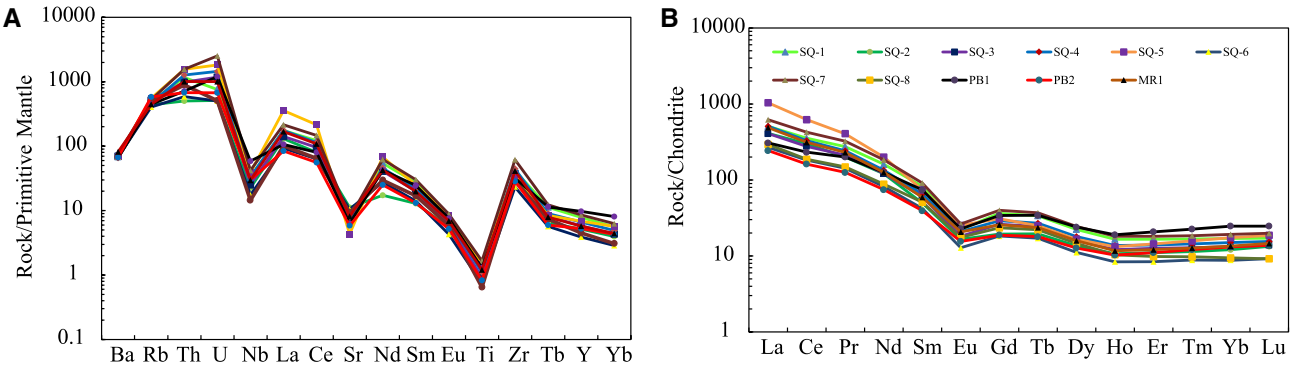

Figure 8. (**a**) Chondrite normalized REE patterns displaying LREE enrichment and distinct negative Eu anomaly and **(b)** primitive mantle normalized trace element distribution pattern showing negative Sr, Nb and Ti anomalies in Granite. Normalizing factors are from Sun and McDonough (1989).

Ba relative to HFSE with slightly low Sr/Y ratio. These granites are characterized by higher thorium (43–133 ppm) and U contents (11–53 ppm) compared to various granitic plutons of eastern Dharwar Craton (Dey *et al.* 2014; Mukherjee *et al.* 2018; Shukla and Ram Mohan 2019). Chondrite-normalized REE patterns exhibit sharp LREE/MREE $[(La/Sm)_N = 4.16 - 13.93]$ and LREE/HREE $[(La/Yb)_N = 12.48 - 59.42]$ with moderate to feeble MREE/HREE $[(Gd/Yb)_N = 1.38-1.77]$ fractionation (figure 8a). The distinct negative Eu anomaly ($Eu/Eu^* = 0.41-0.57$) of these granites reflect on plagioclase fractionation during the magma evolution. On primitive mantle normalized diagram (figure 8b), these granites exhibit distinct enrichment of LILE (Rb, U, La, Ce) and strong negative Nb, Ti and Sr anomalies.

6. Discussions

6.1 *Alteration and elemental mobility*

Several studies have reported that Archean cratons are more prone to alteration due later metamorphism or hydrothermal activity. Therefore, it is essential to evaluate the elemental mobility in the Archean rocks to precisely interpret their geodynamic setting (Ward *et al.* 1992; Polat and

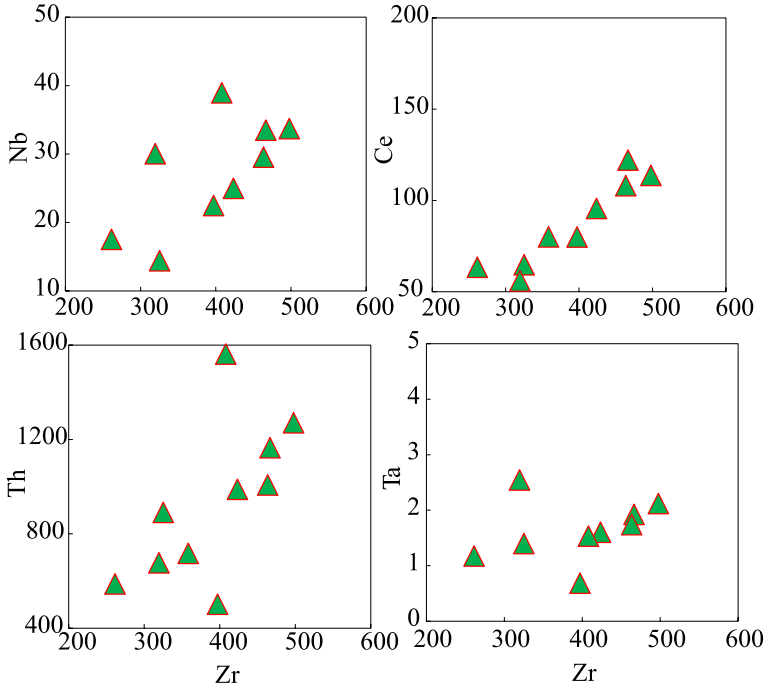

Figure 9. Zr vs. other Trace elements relationship indicating post magmatic alteration effect and the positive correlation and coherent pattern showing the primary igneous characters for these granites.

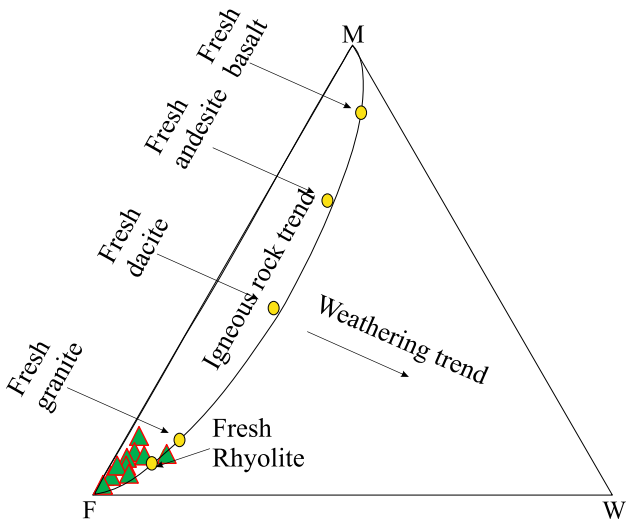

Figure 10. MFW ternary diagram (after Ohta and Arai 2007) showing that the granitoids plot along the igneous trend indicating their unaltered nature.

Hofmann 2003; Szilas and Garde 2013). Low Spitz-Darling index values (Al_2O_3/Na_2O<10; Spitz and Darling 1978) and loss-on-ignition (<2%) along with coherent trace and REE patterns indicate that the studied granites are retaining their primary igneous characters and least affected by alteration. Zr is considered as one of the least altered elements which may be altered in some special situations (e.g., acid-sulphate conditions; presence of F) and thus used as an important index to deduce the alteration of the rocks (Pearce and Peate 1995; Winchester and Floyd 1977). The HFSE (Nb, Ce, Th, Ta) show a positive correlation with Zr (figure 9) indicating that these elements are not mobilized due to alteration (Li and Wei 2017). Major element relationship between K_2O/Na_2O and SiO_2, CaO, MgO, Al_2O_3, Fe_2O_3 and LOI are also indicating their unaltered nature and the primary magmatic chemistry of these rocks (Páez *et al.* 2010; figure not shown). On mafic–felsic–weathering index diagram (figure 10), these granites are concentrated in left base which indicates their unaltered nature (Ohta and Arai 2007). The above geochemical characteristics reflect their least altered or near primary igneous nature which are not changed by the secondary alteration or metamorphism.

6.2 *Characterization of granites and their source*

The petrographic and geochemical signatures characterise the studied rocks as granites which are classified on the basis of three geochemical parameters such as Fe* [$FeO^{(t)}/(FeO^{(t)}+MgO)$], modified alkali-lime index (MALI; Na_2O+K_2O-CaO) and the aluminium saturation index (ASI; [Al/(Ca−1.67P+Na+K)]; Shand 1943). The granites are showing high Fe* (0.78–0.88) and

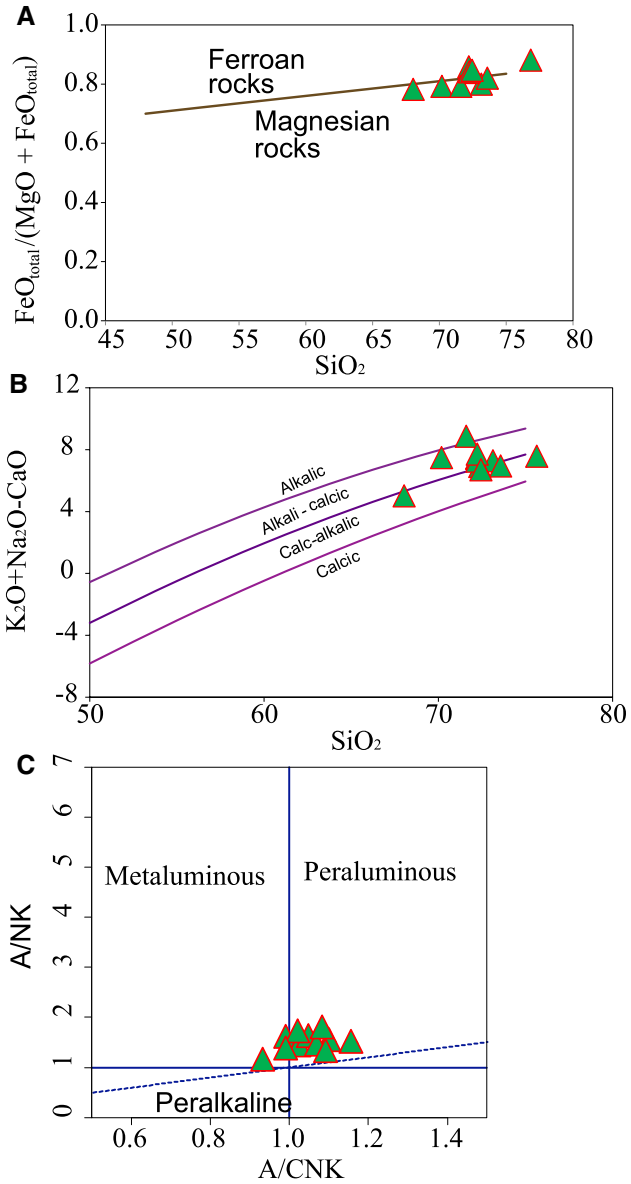

Figure 11. (**a**) SiO_2 vs. Ferroan Index (after Frost *et al.* 2001) showing magnesian nature of granites SiO_2 *vs.* MALI-index diagram (after Frost *et al.* 2001) showing alkali-calcic to alkalic character. (**b**, **c**) Molar A/CNK vs. A/NK diagram showing the peraluminous to metaluminous nature of the studied granites (after Shand 1943).

occupying the magnesian field on $FeO^{(t)}/(FeO^{(t)}+MgO)$ vs. SiO_2 diagram (Frost *et al.* 2001; figure 11a). The high modified alkali lime index (MALI index; 5.02–8.87) of these granites indicate the alkali-calcic to alkalic nature (figure 11b). These granites are strongly peraluminous to metaluminous (figure 11c), with moderate Alumina Saturation Index (ASI) ranging from 0.86 to 1.11 indicating the role of plagioclase in their genesis. The magnesian character imply an oxidizing source for these granites (Frost and Frost 2008). On the basis of geochemical characteristics,

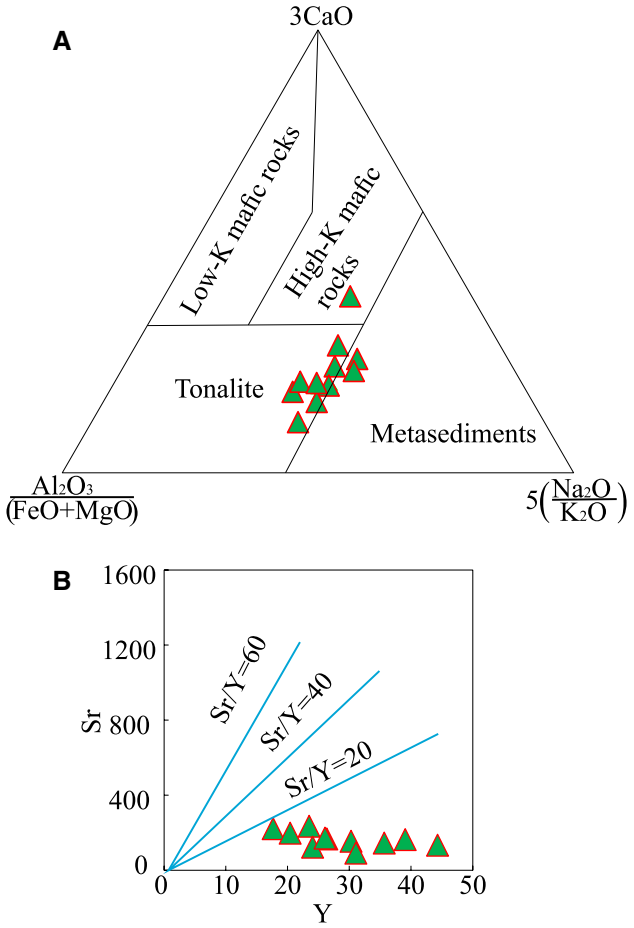

Figure 12. (**a**) Ternary diagram $Al_2O_3/(FeO_t+MgO)$; 3*CaO; 5*(K_2O/Na_2O) showing the possible sources of the granite, (**b**) Sr vs. Y relationship indicating the lower pressure regime for the emplacement of these granites (Nandy *et al.* 2019).

Bonin (2007) identified different types of granites such as S, I, A and M. The S-types are particularly derived from the partial melting of metasediments, while the I-type are typically metaluminous to peraluminous in nature and formed by the partial melting of igneous rock and M-type granites are directly formed by the partial melting of subducted crust or fractionation of basaltic magma. A-type granites display peraluminous to peralkaline characteristics which are slightly different from the earlier varieties because of their genesis at extensional anorogenic setting (Eby 1992; Poitrasson *et al.* 1994; Mushkin *et al.* 2003; Bonin 2007). Therefore, the peraluminous to metaluminous character and presence of inherited igneous zircons (euhedral shape) discard the sedimentary source for the genesis of these granites (Joshi *et al.* 2017) and conforms the I-type which appears to have been derived by the partial melting of older TTG and granitoids at shallow crustal depth (Moyen 2011). Their alkali-calcic to alkalic nature, narrow

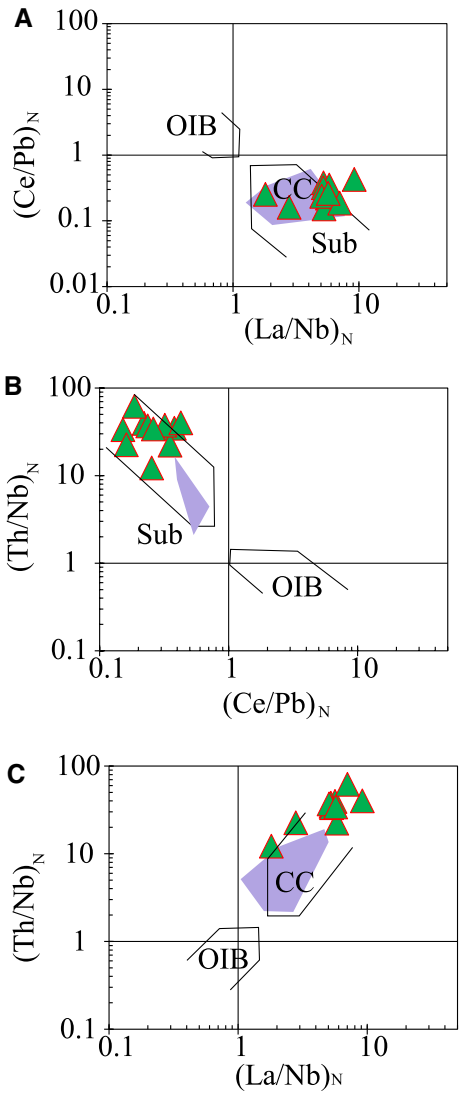

Figure 13. (**a**, **b**, **c**). Relationships between Th/Nb, La/Nb and Ce/Pb of showing their subduction origin for the studied granite. Normalization values after McDonough and Sun (1995). Compositional fields after Moreno *et al.* (2016). Abbreviations. CA: Continental Arcs; CC: Continental Crust; OIB: Ocean Island Basalts; Sub: subduction-related magmatic suites.

range of MALI Index, low Fe-number implying their similarity with the I-type Cordilleran granite (Chappel and White 2001; Frost *et al.* 2001). On the discrimination diagram, these granites are concentrating in the tonalite filed (Laurent *et al.* 2014) from which it is evident that the source rock for the granites are the older TTG gneisses of EDC (figure 12a). These granites are showing distinct negative europium anomalies, enriched LREE and flat to moderately depleted HREE patterns along with low Sr/Y ratio (Nandy *et al.* 2019, figures 12b and 8) which collectively indicate moderate to low pressure melting of the TTG source with plagioclase in the residue (Nandy *et al.* 2019). Moreno *et al.* (2014, 2016) have conducted systematic study on trace element ratios to infer the magma source of the granites. The relationship among Th/Nb, La/Nb, Ce/Pb reflect the continental crust or subduction related source which is supported by the Nb/Ta ratio (7–23) close to the continental crust (Nb/Ta = 11–12; Green, 1995; figure 13a, b, c). Therefore, the studied granites are geochemically I-type, peraluminous to metaluminous and derived from partial melting of older TTG gneisses which is coinciding with the other granites of EDC (Dey *et al.* 2012, 2014, 2017; Ram Mohan *et al.* 2013; Nandy *et al.* 2019).

6.3 *Petrogenesis of Hyderabad granitic batholith of EDC*

In the Dharwar Craton, Archean–Proterozoic boundary is manifested by the Neoarchean granitic activity which is an important event of crustal melting and differentiation process (Subbarao *et al.* 1998). In general, the granites are characterized by a wide spectrum of geochemistry based on source, degree of partial melting and fractional crystallization (DePaolo 1981; Thompson and Connolly 1995; Ray *et al.* 2011). In general, younger granites are formed through the intracrustal melting of older crust (TTG and gneisses) and subsequent fractional crystallization which is also evidenced from the granites of eastern Dharwar Craton (Sylvester 1994; Smithies and Witt 1997; Dey *et al.* 2003, 2009, 2012; Mikkola *et al.* 2012; Pahari *et al.* 2019). Prominent negative Europium anomaly, high Sr, Rb, Rb/Sr and low Sr/Y indicates moderate to low pressure partial melting of pre-existing TTG with residual plagioclase in the source. The strong negative Eu and Sr anomalies in the studied granites indicate early fractionation of plagioclase from the melt (Rollinson 1993) which is corroborated from the major and trace element relationship with their typical magmatic trend (figure 6). Based on the negative to positive εNd values, earlier workers suggested that the granites of EDC are formed by the partial melting of TTGs with lower crustal residence time of the source (Jayananda *et al.* 2000; Martin *et al.* 2005). According to Martin (1999), the higher abundance of Cr, Ni and Mg# indicates deeper depth of melting and probable interaction of mantle peridotite and felsic material that are derived by the melting of rutile bearing hydrous basaltic crust in a subduction zone

environment. In our study, the granites with a lower Cr, Ni contents and Mg# discard the mantle influence and supports the intracrustal melting in their genesis. Geochemically, the studied granites are similar to Kadiri leucogranites (Dey *et al.* 2014) which are evolved from a heterogenous source occurring as remnants of older TTG within the EDC (Jayananda *et al.* 2000; Bidyananda *et al.* 2011). Through REE modelling, Nandy *et al.* (2019) have suggested the derivation of Tsundapalli granites of EDC from the Archean TTG source. Similar type of late Archean granites are also reported from the Yalgran Craton, Australia (Champion and Sheraton 1997), North China (Jahn *et al.* 1988), Superior Province, Canada (Shirey and Hanson 1986; Meldrum *et al.* 1997) and Bastar Craton, India (Singh *et al.* 2019). Keeping in view of the resemblances with other counterparts of EDC, it is suggested that the studied granites are evolved from the older TTG of Dharwar Craton which are present as remnants at some places.

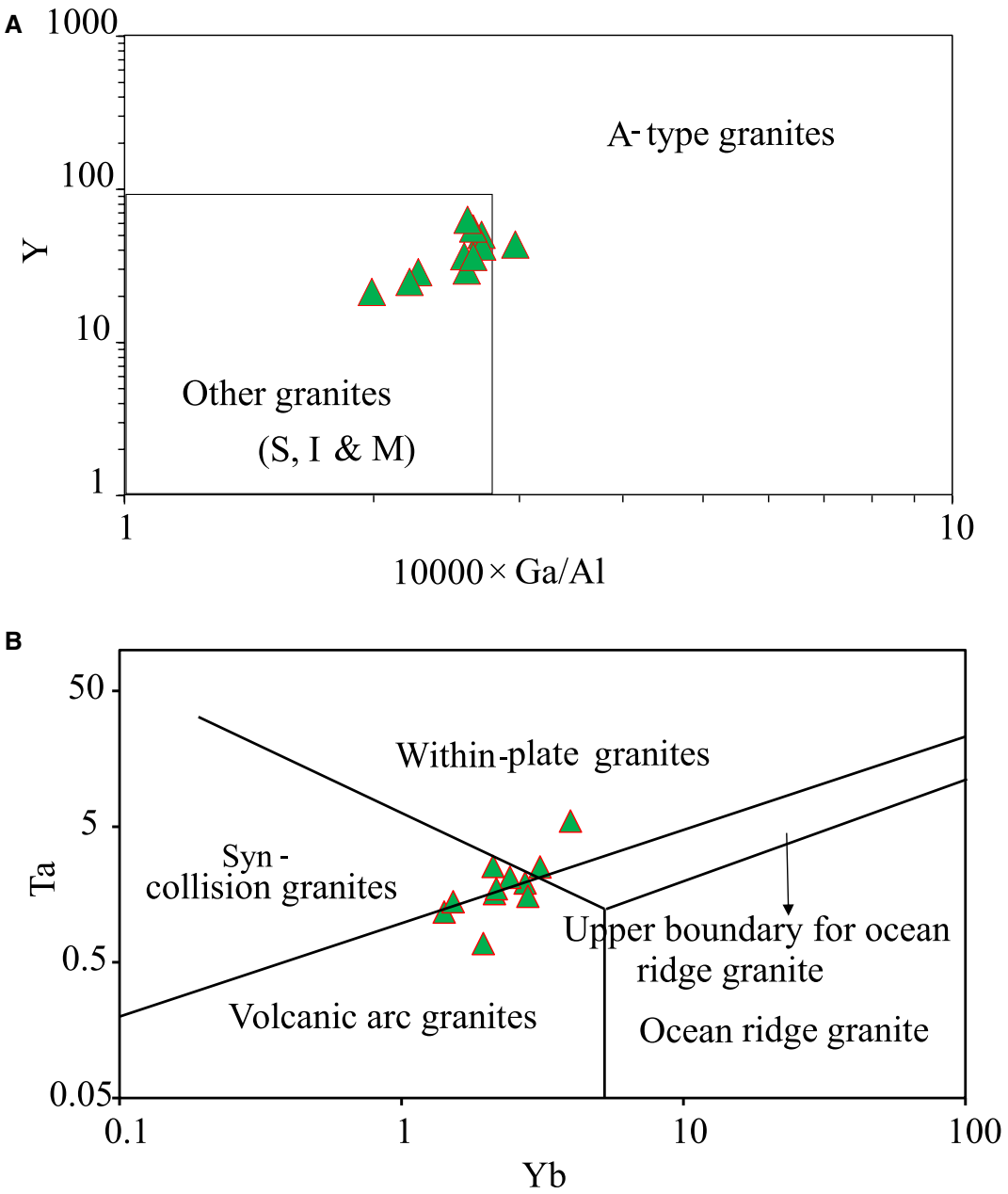

Figure 14. (**a**) Y vs. 10000 X Ga/Al classification plot for A, I, S and M type granites in which the studies samples occupy the field of orogenic type (after Whalen *et al.* 1987); **(b)** Yb vs. Ta tectonic discrimination diagram (after Pearce 1984) syn-collisional volcanic arc affinity of the studied granites.

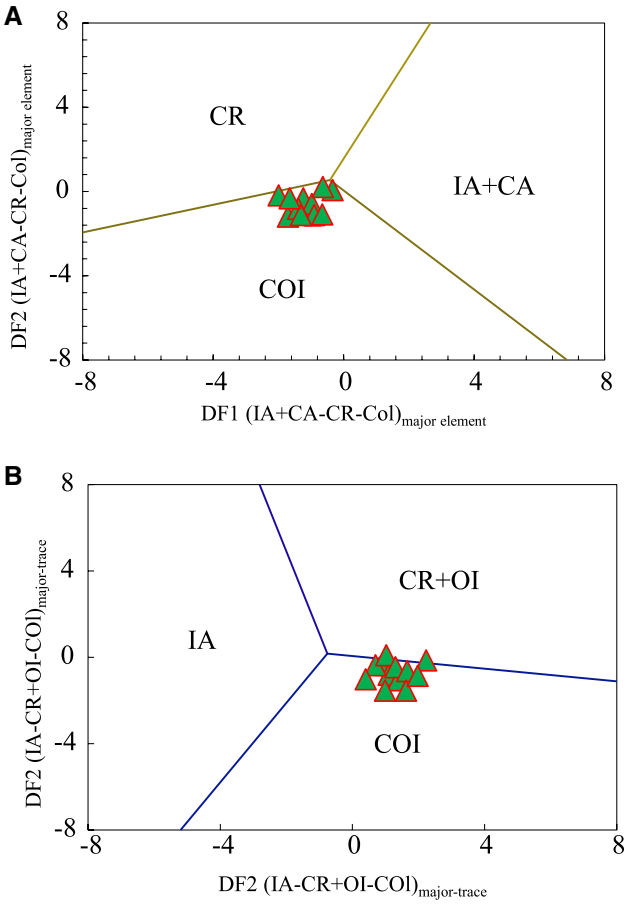

Figure 15. (**a**, **b**) Tectonic discriminant multidimensional diagrams based on ln-transformed ratios of major and immobile trace elements showing the post subduction collisional setting for the studied granites (Verma *et al.* 2012, 2013).

6.4 *Tectonic setting and geodynamic model*

The calc-alkaline affinity, hydrous nature, potash enrichment and other geochemical proxies of the studied granites indicate that these are formed during the late Archean mantle evolutionary phase. Their peraluminous to metaluminous nature along with their geochemistry discard the intraplate or within plate tectonic setting in their evolution and supportive of collisional environment (Harris *et al.* 1986; Turner *et al.* 1992; Downes *et al.* 1997; Ferré *et al.* 1998; Liégeois *et al.* 1998; Debon and Lemmet 1999; Frost *et al.* 2001; Bonin 2004; Clemens *et al.* 2010). Further, these granites are classified as orogenic type (I, S, and M) and their HFSE systematics discriminate them as syncollisional volcanic arc granites (figure 14a, b; Pearce *et al.* 1984; Whalen *et al.* 1987). Based on logarithmic transformation value, Verma *et al.* (2012, 2013) proposed new discriminant function diagram to evaluate the tectonic settings of acidic rocks with more confidence which are mainly the correction of statistical value of the compositional data (Aitchison 1986), natural log ratio transformation of element ratio and application of discordant outlier tests prior to LDA (logarithmic discriminant analysis). These newly log transformed tectonic diagrams are able to decipher four types of tectonic settings – continental rift (CR), island and continental arc (IA+CA), collisional settings (COI) and oceanic island (OI). The

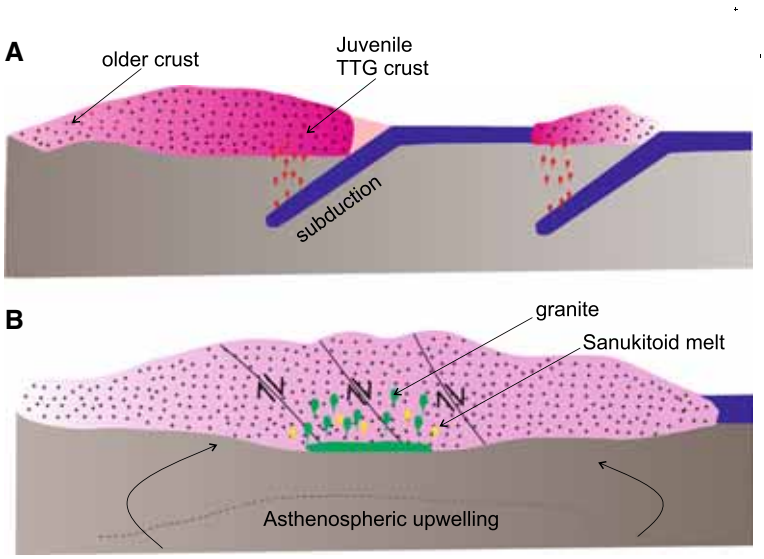

Figure16. Schematic tectonic model explaining **(a)** Juvenile subduction of oceanic crust and generation of TTG crust, **(b)** Generation of metasomatized mantle melts (sanukitoid like), remelting at the base of older TTG crust and intracrustal melting at shallower depth resulted into anatectic granites during collisional orogeny evidenced throughcrustal thickening/granite batholiths in EDC during the Neoarchean timeframe.

studied samples are occupying the collisional field on major and trace element log transformed discriminant diagram (figure 15a, b). Therefore, it is proposed that these granites are mainly formed during the collisional orogeny in EDC. The high potassic nature, lower Fe content and peraluminous to metaluminous character of the studied granites reflect their formation through anatexis of older TTG crust during the collisional stage which marks the cessation of cratonization event during the Neoarchean crustal evolution in the eastern Dharwar Craton (Dey *et al.* 2012, 2014; Nandy *et al.* 2019). On the basis of field and geochemical attributes, a geodynamic model has been proposed for the genesis of the studied granites involving two phases starting from subduction followed by continent–continent collision (Feng and Kerrich 1992; Smithies and Champion 2000; Moyen *et al.* 2003; Whalen *et al.* 2004; Käpyaho *et al.* 2006; Halla *et al.* 2009; Almeida *et al.* 2011, 2013; Dey *et al.* 2014; Nandy *et al.* 2019). In the first phase, the partial melting of hot, eclogitic oceanic slab in a subduction environment generated TTG (figure 16a). With the progress of convergent margin processess in the EDC, the TTG melts metasomatized the sub-continental lithospheric mantle which gave rise the sanukitoid like melts. The heat generated by the sanukitoid melts, initiated remelting of older TTG crust at the base followed by intracrustal melting at shallower depth, generated these late phase anatectic potassic granites in EDC during the Neoarchean time in a syncollisional tectonic framework (figure 16b). These processes led to the closure of the ocean basin and welding of two continental blocks in EDC. The crustal thickening and cratonization processes are evidenced through granitic batholiths that are predominant throughout the EDC.

7. Conclusions

- The studied Hyderabad granites are strongly peraluminous, alkali to alkali-calcic in nature, predominantly consisting of K-feldspar, quartz and biotite with subordinate plagioclase exhibiting porphyritic, intergranular and perthitic textures.
- These granites are characterised by high silica, aluminium, total alkali contents having magnesian to ferroan characteristics, displaying relative enrichment in LREE over HREE and negative Sr, Ti and Nb anomalies.
- The high LILE/HFSE, low Cr, Ni, strong peraluminous to metalauminous characteristics classify them as I-type granites formed in a collisional setting.
- Our studies indicate that the studied Hyderabad granite batholiths are generated in a syn-tectonic/syn-collisional setting through remelting of older TTG crust under the influence of sanukitoid melts (as a heat source) in a subduction zone environment. This process appears to have dominated throughout the Neoarchean time that resulted into granite batholiths marking the cessation of cratonization event in the eastern Dharwar Craton.

Acknowledgements

The authors thank Dr V M Tiwari, Director, CSIR-NGRI for permitting to publish this work. CM acknowledges the funds from Council of Scientific and Industrial Research (CSIR) to National Geophysical Research Institute through MLP 6406-28(CM). The authors are grateful to the two anonymous reviewers for their constructive suggestions, comments, and Prof. Rajneesh Bhutani for efficient editorial handling. Drs M Satyanarayanan, S S Sawant, and A K Krishna are acknowledged for providing the geochemical data. These studies belong to the MSc dissertation work of Mr. Prasanth. Dr Devleena and Mr. Prasanth thank the Head, Centre for Earth, Ocean & Atmospheric Sciences (CEOAS), University of Hyderabad for his support and encouragement. Mr. Arijit Pahari acknowledges the DST INSPIRE Fellowship for pursuing the PhD programme at NGRI.

References

Aitchison J 1986 *The Statistical Analysis of Compositional Data*; Chapman and Hall, London.

Almeida J A C, Dall'Agnol R, Oliveira M A, Macambira M J B, Pimentel M M, Rämö O T, Guimarães F V and Leite A A S 2011 Zircon geochronology, geochemistry and origin of the TTG suites of the Rio Maria granite–greenstone terrane: Implications for the growth of the Archean crust of the Carajás Province, Brazil; *Precamb. Res.* **187** 201–221.

Almeida J A C, Dall'Agnol R and Leite A A S 2013 Geochemistry and zircon geochronology of the Archean granite suites of the Rio Maria granite–greenstone terrane, Carajás Province, Brazil; *J. South Am. Earth Sci.* **42** 103–126.

Anjaneyulu M, Nagaraju K and Reddy I P 2019 Petrological and geochemical studies of precambrian granitoids from cherlapally area, Nalgonda district, Telangana state, India; *J. Appl. Geochem.* **21** 311–316.

Balakrishnan S, Hansen G N and Rajamani V 1990 Pb and Nd isotope constraints on the origin of high Mg and tholeiitic amphibolites, Kolar schist belt, southern India; *Contrib. Mineral. Petrol.* **107** 279–292.

Balakrishnan S, Rajamani V and Hanson G N 1999 U–Pb ages for zircon and titanite from the Ramagiri area, southern India: Evidence for accretionary origin of the eastern Dharwar craton during the late Archean; *J. Geol.* **107** 69–86.

Barnes S J and Van Kranendonk M J 2014 Archean andesites in the east Yilgarn craton, Australia: Products of plume-crust interaction? *Lithosphere* **6** 80–92.

Bidyananda M, Goswami J N and Srinivasan R 2011 Pb–Pb zircon ages of Archaean metasediments and gneisses from the Dharwar craton, southern India: Implications for the antiquity of the eastern Dharwar craton; *J. Earth Syst. Sci.* **120** 643–661.

Bonin B 2004 Do coeval mafic and felsic magmas in post-collisional to within-plate regimes necessarily imply two contrasting, mantle and crustal, sources? A review; *Lithos* **78** 1–24.

Bonin B 2007 A-type granites and related rocks: evolution of a concept, problems and prospects; *Lithos* **97** 1–29.

Chadwick B, Vasudev V N and Hegde G V 2000 The Dharwar craton, southern India, interpreted as the result of Late Archaean oblique convergence; *Precamb. Res.* **99** 91–111.

Champion D C and Sheraton J W 1997 Geochemistry and Nd isotope systematics of Archaean granites of the Eastern Goldfields, Yilgarn Craton, Australia: implications for crustal growth processes; *Precamb. Res.* **83** 109–132.

Chappel B W and White A J R 2001 Two contrasting granite types: 25 years later; *Aust. J. Earth Sci.* **48** 489–499.

Chardon D and Jayananda M 2008 Three-dimensional field perspective on deformation, flow, and growth of the lower continental crust (Dharwar Craton, India); *Tectonics* **27** 1–15.

Clemens J D, Belcher R W and Kisters A F M 2010 The Heerenveen batholith, Barberton Mountain Land, South Africa: Mesoarchaean, potassic, felsic magmas formed by melting of an ancient subduction complex; *J. Petrol.* **51** 1099–1120.

Condie K C 1981 *Archean Greenstone Belts*; Vol. 3, Elsevier, Amsterdam.

Condie K C 1989 Geochemical changes in baslts and andesites across the Archean–Proterozoic boundary: Identification and significance; *Lithos* **23** 1–18.

Condie K C 2000 Episodic continental growth models: afterthoughts and extensions; *Tectonophys.* **322** 153–162.

Condie K C and Kroner A 2013 The building blocks of continental crust: Evidence for a major change in the tectonic setting of continental growth at the end of the Archean; *Gondwana Res.* **23** 394–402.

Crawford A R 1969 Reconnaissance Rb–Sr dating of the Precambrian rocks of southern peninsular India; *J. Geol. Soc. India* **10** 117–166.

Debon F and Lemmet M 1999 Evolution of Fe/Mg ratios in Late Variscan plutonic rocks from the External Crystalline Massif of the Alps (France, Italy, Switzerland); *J. Petrol.* **40** 1151–1185.

De Paolo D J 1981 Trace element and isotopic effects of combined wall rock assimilation and fractional crystallization; *Earth Planet. Sci. Lett.* **53** 189–202.

Dey S, Gajapathi Rao R, Gorikhan R A, Veerabhaskar D and Sunil Kumar M K 2003 Geochemistry and origin of northern Closepet Granite from Gudur-Guledagudda area, Bagalkot district, Karnataka; *J. Geol. Soc. India* **62** 152–168.

Dey S, Rai A K and Chaki A 2009 Geochemistry of granitoids of Bilgi area, northern part of eastern Dharwar craton, southern India—example of transitional TTGs derived from depleted source; *J. Geol. Soc. India* **73** 854–870.

Dey S, Pandey U K, Rai A K and Chaki A 2012 Geochemical and Nd isotope constraints on petrogenesis of granitoids from NW part of the eastern Dharwar craton: possible implications for late Archaean crustal accretion; *J. Asian Earth Sci.* **45** 40–56.

Dey S, Nandy J, Choudhary A K, Liu Y and Zong K 2014 Origin and evolution of granitoids associated with the Kadiri greenstone belt, eastern Dharwar craton: a history of orogenic to anorogenic magmatism; *Precamb. Res.* **246** 64–90.

Dey S, Halla J, Kurhila M, Nandy J, Heilimo E and Pal S 2017 Geochronology of Neoarchean granitoids of the NW eastern Dharwar craton: Implications for crust formation; *Geol. Soc. London Spec. Publ.* **449** 89–121.

Downes H, Shaw A, Williamson B J and Thirlwall M F 1997 Sr, Nd and Pb isotope geochemistry of the Hercynian granodiorites and monzogranites, Massif Central, France; *Chem. Geol.* **136** 99–122.

Eby G N 1992 Chemical subdivision of the A-type granitoids: petrogenetic and tectonic implications; *Geol*ogy **20** 641–644.

Feng R and Kerrich R 1992 Geochemical evolution of granitoids from the Archean Abitibi Southern Volcanic Zone and the Pontiac subprovince, Superior Province, Canada: implications for tectonic history and source regions; *Chem. Geol.* **98** 23–70.

Ferré E C, Caby R, Peucat J J, Capdevila R and Monié P 1998 Pan-African, post-collisional, ferro-potassic granite and quartz–monzonite plutons of Eastern Nigeria; *Lithos* **45** 255–279.

Fliedner M M and Klemperer S L 2000 Crustal structure transition from oceanic arc to continental arc, eastern Aleutian Islands and Alaska Peninsula; *Earth Planet. Sci. Lett.* **179** 567–579.

French J E and Heaman L M 2010 Precise U–Pb dating of Paleoproterozoic mafic dyke swarms of the Dharwar craton, India: implications for the existence of the Neoarchean supercraton Sclavia; *Precamb. Res.* **183** 416–441.

Frost B R and Frost C D 2008 A geochemical classification for feldspathic igneous rocks; *J. Petrol.* **49** 1955–1969.

Frost B R, Barnes C G, Collins W J, Arculus R J, Ellis D J and Frost C D 2001 A geochemical classification for granitic rocks; *J. Petrol.* **42** 2033–2048.

Gastil G 1960 Continents and mobile belts in the light of mineral dating; *Int. Geol. Congress* **9** 162–169.

Goutham M R, Sandhya R, Rao B M, Patil S K and Murthy B V S 2010 Rock magnetic and palaeomagnetic study of the

Archaean granites from Hyderabad, India; *J. Indian Geophys. Union* **14** 67–74.

Green T H 1995 Significance of Nb/Ta as an indicator of geochemical processes in the crust-mantle system; *Chem. Geol.* **120** 347–359.

GSI 1995 District resource map of Nalgonda region of EDC; Geological Survey of India, Kolkata.

Guitreau M, Mukasa S B, Loudin L and Krishnan S 2017 New constraints on the early formation of the Western Dharwar Craton (India) from igneous zircon U-Pb and Lu-Hf isotopes; *Precamb. Res.* **302** 33–49.

Halla J, van Hunen J, Heilimo E and Hölttä P 2009 Geochemical and numerical constraints on Neoarchean plate tectonics; *Precamb. Res.* **174** 155–162.

Harris N B W, Pearce J A and Tindle A G 1986 Geochemical characteristics of collision zone magmatism; *Geol. Soc. London Spec. Publ.* **19** 67–81.

Heilimo E, Halla J and Huhma H 2011 Single-grain zircon U–Pb age constraints of the western and eastern sanukitoid zones in the Finnish part of the Karelian Province; *Lithos* **121** 87–99.

Huppert H E and Sparks R S J 1988 The generation of granitic magmas by intrusion of basalt into continental crust; *J. Petrol.* **29** 599–624.

Irvine T N J and Baragar W R A 1971 A guide to the chemical classification of the common volcanic rocks; *Canadian J. Earth Sci.* **8** 523–548.

Jahn B M, Auvray B, Shen Q H, Liu D Y, Zhang Z Q, Dong Y J and Mace J 1988 Archean crustal evolution in China: the Taishan complex, and evidence for juvenile crustal addition from long-term depleted mantle; *Precamb. Res.* **38** 381–403.

Janardhan A S, Newton R C and Hansen E C 1982 The transformation of amphibolite facies gneiss to charnockite in southern Karnataka and northern Tamil Nadu, India; *Contrib. Mineral. Petrol.* **79** 130–149.

Jayananda M, Martin H, Peucat J J and Mahabaleswar B 1995 Late Archaean crust-mantle interactions: Geochemistry of LREE-enriched mantle derived magmas. Example of the Closepet batholith, southern India; *Contrib. Mineral. Petrol.* **119** 314–329.

Jayananda M, Moyen J F, Martin H, Peucat J J, Auvray B and Mahabaleswar B 2000 Late Archaean (2550–2520 Ma) juvenile magmatism in the Eastern Dharwar craton, southern India: Constraints from geochronology, Nd–Sr isotopes and whole rock geochemistry; *Precamb. Res.* **99** 225–254.

Jayananda M, Chardon D, Peucat J J and Capdevila R 2006 2.61 Ga potassic granites and crustal reworking in the western Dharwar craton, southern India: Tectonic, geochronologic and geochemical constraints; *Precamb. Res.* **150** 1–26.

Jayananda M, Kano T, Peucat J J and Channabasappa S 2008 3.35 Ga komatiite volcanism in the western Dharwar craton, southern India: Constraints from Nd isotopes and whole-rock geochemistry; *Precamb. Res.* **162** 160–179.

Jayananda M, Peucat J J, Chardon D, Rao B K, Fanning C M and Corfu F 2013 Neoarchean greenstone volcanism and continental growth, Dharwar craton, southern India: Constraints from SIMS U–Pb zircon geochronology and Nd isotopes; *Precamb. Res.* **227** 55–76.

Jayananda M, Gireesh R V, Sekhamo K U and Miyazaki T 2014 Coeval felsic and mafic magmas in neoarchean calc-alkaline magmatic arcs, Dharwar Craton, southern India: field and petrographic evidence from mafic to Hybrid magmatic enclaves and synplutonic mafic dykes; *J. Geol. Soc. India* **84** 5–28.

Jayananda M, Santosh M and Aadhiseshan K R 2018 Formation of Archean (3600–2500 Ma) continental crust in the Dharwar Craton, southern India; *Earth Sci. Rev.* **181** 12–42.

Jayananda M, Guitreau M, Thomas T T, Martin H, Aadhiseshan K R, Gireesh R V, Peucat J J and Satyanarayanan M 2019 Geochronology and geochemistry of Meso-to-Neoarchean magmatic epidote-bearing potassic granites, western Dharwar Craton (Bellur–Nagamangala–Pandavpura corridor), southern India: Implications for the successive stages of crustal reworking and cratonization; *Geol. Soc. London Spec. Publ.* **489** 489–2018.

Joshi K B, Bhattacharjee J, Rai G, Halla J, Ahmad T, Kurhila M and Choudhary A K 2017 The diversification of granitoids and plate tectonic implications at the Archaean–Proterozoic boundary in the Bundelkhand Craton, Central India; *Geol. Soc. London Spec. Publ.* **449** 123–157.

Käpyaho A, Mänttäri I and Huhma H 2006 Growth of Archaean crust in the Kuhmo district, Eastern Finland: U–Pb and Sm–Nd isotope constraints on plutonic rocks; *Precamb. Res.* **146** 95–119.

Krishna A K, Murthy N N and Govil P K 2007 Multi-element analysis of soils by wavelength-dispersive X-ray fluorescence spectrometry; *Atomic Spectrosc. Norwalk Conn.* **28** 202.

Krogstad E J, Hanson G N and Rajamani V 1991 U–Pb ages of zircon and sphene for two gneiss terranes adjacent to the Kolar Schist Belt, South India: evidence for separate crustal evolution histories; *J. Geol.* **99** 801–815.

Laurent O, Martin H, Moyen J F and Doucelance R 2014 The diversity and evolution of late-Archean granitoids: Evidence for the onset of modern-style plate tectonics between 3.0 and 2.5 Ga; *Lith*os **205** 208–235.

Li Z and Wei C 2017 Two types of Neoarchean basalts from Qingyuan greenstone belt, North China Craton: petrogenesis and tectonic implications; *Precamb. Res.* **292** 175–192.

Li S S, Santosh M, Ganguly S, Thanooja P V, Sajeev K, Pahari A and Manikyamba C 2018 Neoarchean microblock amalgamation in southern India: Evidence from the Nallamalai Suture Zone; *Precamb. Res.* **314** 1–27.

Liégeois J P, Navez J, Hertogen J and Black R 1998 Contrasting origin of post-collisional high-K calc-alkaline and shoshonitic versus alkaline and peralkaline granitoids. The use of sliding normalization; *Lithos* **45** 1–28.

Madhusudhan Rao B, Shashidhar D, Narsaiah R and Murthy B V S 2002 Geological significance of magnetic signatures over the granitic region in Osmania University campus, Hyderabad, India; *J. Indian Acad. Geosci.* **45** 39–44.

Maniar P D and Piccoli P M 1989 Tectonic discrimination of granitoids; *Geol. Soc. Am. Bull.* **101** 635–643.

Manikyamba C and Kerrich R 2012 Eastern Dharwar Craton, India: Continental lithosphere growth by accretion of diverse plume and arc terranes; *Geosci. Frontiers* **3** 225–240.

Manikyamba C, Kerrich R, Naqvi S M and Mohan M R 2004a Geochemical systematics of tholeiitic basalts from the 2.7 Ga Ramagiri–Hungund composite greenstone belt, Dharwar craton; *Precamb. Res.* **134** 21–39.

Manikyamba C, Naqvi S M, Mohan M R and Rao T G 2004b Gold mineralisation and alteration of Penakacherla schist belt, India, constraints on Archaean subduction and fluid processes; *Ore Geol. Rev.* **24** 199–227.

Manikyamba C, Naqvi S M, Rao D S, Mohan M R, Khanna T C, Rao T G and Reddy G L N 2005 Boninites from the Neoarchaean Gadwal greenstone belt, Eastern Dharwar craton, India: Implications for Archaean subduction processes; *Earth Planet. Sci. Lett.* **230** 65–83.

Manikyamba C, Kerrich R, Khanna T C, Krishna A K and Satyanarayanan M 2008 Geochemical systematics of komatiite–tholeiite and adakitic-arc basalt associations: the role of a mantle plume and convergent margin in formation of the Sandur Superterrane, Dharwar craton, India; *Lithos* **106** 155–172.

Manikyamba C, Kerrich R, Khanna T C, Satyanarayanan M and Krishna A K 2009 Enriched and depleted arc basalts, with Mg-andesites and adakites: a potential paired arc—back-arc of the 2.6 Ga Hutti greenstone terrane, India; *Geochim. Cosmochim. Acta* **73** 1711–1736.

Manikyamba C, Kerrich R, Polat A, Raju K, Satyanarayanan M and Krishna A K 2012 Arc picrite–potassic adakitic—shoshonitic volcanic association of the Neoarchean Sigegudda Greenstone Terrane, Western Dharwar Craton: transition from arc wedge to lithosphere melting; *Precamb. Res.* **212** 207–224.

Manikyamba C, Kerrich R, Polat A and Saha A 2013 Geochemistry of two stratigraphically-related ultramafic (komatiite) layers from the Neoarchean Sigegudda greenstone terrane, Western Dharwar Craton, India: evidence for compositional diversity in Archean mantle plumes; *Lithos* **177** 120–135.

Manikyamba C, Santosh M, Kumar B C, Rambabu S, Tang L, Saha A, Khelen A C, Ganguly S, Singh T D and Rao D S 2016 Zircon U–Pb geochronology, Lu–Hf isotope systematics, and geochemistry of bimodal volcanic rocks and associated granitoids from Kotri Belt, Central India: Implications for Neoarchean–Paleoproterozoic crustal growth; *Gondwana Res.* **38** 313–333.

Manikyamba C, Ganguly S, Santosh M and Subramanyam K S V 2017 Volcano-sedimentary and metallogenic records of the Dharwar greenstone terranes, India: window to Archean plate tectonics, continent growth, and mineral endowment; *Gondwana Res.* **50** 38–66.

Martin H 1993 The mechanisms of petrogenesis of the Archaean continental crust-comparison with modern processes; *Lithos* **30** 373–388.

Martin H 1999 Adakitic magmas: modern analogues of Archaean granitoids; *Lithos* **46** 411–429.

Martin H, Smithies R H, Rapp R, Moyen J F and Champion D 2005 An overview of adakite, tonalite–trondhjemite–granodiorite (TTG), and sanukitoid: Relationships and some implications for crustal evolution; *Lithos* **79** 1–24.

McDonough W F and Sun S S 1995 The composition of the Earth; *Chem. Geol.* **120** 223–253.

Meldrum A, Abdel-Rahman A F, Martin R F and Wodicka N 1997 The nature, age and petrogenesis of the Cartier Batholith, northern flank of the Sudbury Structure, Ontario, Canada; *Precamb. Res.* **82** 265–285.

Mikkola P, Lauri L S and Kapyaho A 2012 Neoarchean leucogranitoids of the Kianta Complex, Karelian Province, Finland: source characteristics and processes responsible for the observed heterogeneity; *Precamb. Res.* **206–207** 72–86.

Moreno J A, Molina J F, Montero P, Anbar M A, Scarrow J H, Cambeses and Bea F 2014 Unraveling sources of A-type magmas in juvenile continental crust: Constraints from compositionally diverse Ediacaran post-collisional granitoids in the Katerina Ring Complex, southern Sinai, Egypt; *Lithos* **192** 56–85.

Moreno J A, Molina J F, Bea F, Anbar M A and Montero P 2016 Th–REE and Nb–Ta accessory minerals in post-collisional Ediacaran felsic rocks from the Katerina Ring Complex S. Sinai, Egypt: An assessment for the fractionation of Y/Nb, Th/Nb, La/Nb and Ce/Pb in highly evolved A-type granites; *Lithos* **258** 173–196.

Moyen J F 2011 The composite Archaean grey gneisses: petrological significance, and evidence for a non-unique tectonic setting for Archaean crustal growth; *Lithos* **123** 21–36.

Moyen J-F, Martin H and Jayananda M 2001 Multi-element geochemical modelling of crust–mantle interactions during late-Archaean crustal growth: the Closepet granite (south India); *Precamb. Res.* **112** 87–105.

Moyen J F, Martin H, Jayananda M and Auvray B 2003 Late Archaean granites: a typology based on the Dharwar Craton (India); *Precamb. Res.* **127** 103–123.

Mukherjee S, Ghosh G, Das K, Bose S and Hayasaka Y 2018 Geochronological and geochemical signatures of the granitic rocks emplaced at the north-eastern fringe of the Eastern Dharwar Craton, south India: Implications for late Archean crustal growth; *Geol. J.* **53** 781–1801.

Murthy N G K 1995 Proterozoic mafic dykes in southern peninsular India; *Geol. Soc. India Memoir* **33** 81–98.

Mushkin A, Navon O, Halicz L, Hartmann G and Stein M 2003 The petrogenesis of A-type magmas from the Amram Massif, southern Israel; *J. Petrol.* **44** 815–832.

Nandy J, Dey S and Heilimo E 2019 Neoarchaean magmatism through arc and lithosphere melting: evidence from Eastern Dharwar Craton; *Geol. J.* https://doi.org/10.1002/gj.3498.

Naqvi S M and Rogers J J W 1987 *Precambrian Geology of India*; Oxford University Press, New York.

Narshimha C H, Reddy U V B, Sesha Sai V V and Subramanyam K S V 2018 Petrological and geochemical characterisation of the Punugodu Granite Pluton, Nellore Schist Belt; Implications for proterozoic anorogenic granite magmatism in the Eastern Dharwar Craton, southern India; *J. Indian Geophys. Union* **22** 187–97.

O'connor J T 1965 A classification for quartz-rich igneous rocks based on feldspar ratios; *US Geol. Surv. Prof. Paper B* **525** 79–84.

Ohta T and Arai H 2007 Statistical empirical index of chemical weathering in igneous rocks: a new tool for evaluating the degree of weathering; *Chem. Geol.* **240** 280–297.

Páez G N, Ruiz R, Guido D M, Jovic S M and Schalamuk I B 2010 The effects of K-metasomatism in the Bahía Laura Volcanic Complex, Deseado Massif, Argentina: petrologic and metallogenic consequences; *Chem. Geol.* **273** 300–313.

Pahari A, Tang L, Manikyamba C, Santosh M, Subramanyam K S V and Ganguly S 2019 Meso-Neoarchean magmatism and episodic crustal growth in the Kudremukh–Agumbe granite-greenstone belt, Western Dharwar Craton, India; *Precamb. Res.* **323** 16–54.

Pandey O P, Agrawal P K and Chetty T R K 2002 Unusual lithospheric structure beneath the Hyderabad granitic region, eastern Dharwar craton, south India; *Phys. Earth Planet. Int.* **130** 59–69.

Pearce J A, Harris N B and Tindle A G 1984 Trace element discrimination diagrams for the tectonic interpretation of granitic rocks; *J. Petrol.* **25** 956–983.

Pearce J A and Peate D W 1995 Tectonic implications of the composition of volcanic arc magmas; *Ann. Rev. Earth Planet. Sci.* **23** 251–285.

Peccerillo A and Taylor S R 1976 Geochemistry of Eocene calc-alkaline volcanic rocks from the Kastamonu area, northern Turkey; *Contrib. Mineral. Petrol.* **58** 63–81.

Peucat J J, Mahabaleswar B and Jayananda M 1993 Age of younger tonalitic magmatism and granulitic metamorphism in the south Indian transition zone (Krishnagiri area): Comparison with older peninsular gneisses from the Gorur–Hassan area; *J. Metamophr. Geol.* **11** 879–888.

Peucat J J, Bouhallier H, Fanning C M and Jayananda M 1995 Age of the Holenarsipur greenstone belt, relationships with the surrounding gneisses (Karnataka, south India); *J. Geol.* **103** 701–710.

Peucat J J, Jayananda M, Chardon D, Capdevila R, Fanning C M and Paquette J L 2013 The lower crust of the Dharwar Craton, southern India: Patchwork of Archean granulitic domains; *Precamb. Res.* **227** 4–28.

Poitrasson F, Pin C, Duthou J L and Platevoet B 1994 Aluminous subsolvus anorogenic granite genesis in the light of Nd isotopic heterogeneity; *Chem. Geol.* **112** 199–219.

Polat A and Hofmann A W 2003 Alteration and geochemical patterns in the 3.7–3.8 Ga Isua greenstone belt, West Greenland; *Precamb. Res.* **126** 197–218.

Praveen K, Anjaneyulu M, Narshimha C and Reddy U V B 2018 Petrology and geochemistry data of the precambrian granitoids from the Hyderabad area, part of Eastern Dharwar Craton, Telangana state, India; *Data in Brief* **21** 1909–1917.

Radhakrishna B P 1983 Archaean granite-greenstone terrain of the south Indian Shield in Precambrian of south India; *Geol. Soc. India Memoir* **4** 1–46.

Radhakrishna T, Balasubramonian G, Joseph M and Krishnendu N R 2004 Mantle processes and geodynamics: Inferences from mafic dykes of south India; Earth System Science and Natural Resources Management, CESS Silver Jubilee Compendium, pp. 3–25.

Ramakrishnan M and Vaidyanadhan R 2010 *Geology of India*; 2nd edn, vol. 1. Geological Society of India, Bangalore.

Ram Mohan M, Piercey S J, Kamber B S and Sarma D S 2013 Subduction related tectonic evolution of the Neoarchean eastern Dharwar Craton, southern India: New geochemical and isotopic constraints; *Precamb. Res.* **227** 204–226.

Rao, N V C, Wu Yuan F, Mitchell R H, Li Li Q and Lehmann B 2013 Mesoproterozoic U–Pb ages, trace elements and Sr–Nd isotopic composition of perovskite from kimberlites of the eastern Dharwar Craton, southern India: Distinct mantle sources and a widespread 1.1 Ga tectono-magmatic event; *Chem. Geol.* **353** 48–64.

Ray J, Saha A, Ganguly S, Balaram V, Krishna A K and Hazra S 2011 Geochemistry and petrogenesis of Neoproterozoic Mylliem granitoids, Meghalaya Plateau, northeastern India; *J. Earth Syst. Sci.* **120** 459–473.

Reymer A and Schubert G 1986 Rapid growth of some major segments of continental crust; *Geology* **14** 299–302.

Rollinson H R 1993 A terrane interpretation of the Archaean Limpopo Belt; *Geol. Mag.* **130** 755–765.

Samal A K and Srivastava R K 2014 Petrographic and XRD studies on a new occurrence of molybdenite within late Archaean mafic enclaves near Hyderabad, eastern Dharwar craton, India; *Curr. Sci.* **106** 364–367.

Santosh M, Shaji E, Tsunogae T, Mohan M R, Satyanarayanan M and Horie K 2013 Suprasubduction zone ophiolite from Agali hill: petrology, zircon SHRIMP U–Pb geochronology, geochemistry and implications for Neoarchean plate tectonics in southern India; *Precamb. Res.* **231** 301–324.

Sarma D S, Fletcher I R, Rasmussen B, McNaughton N J, Mohan M R and Groves D I 2011 Archaean gold mineralization synchronous with late cratonization of the Western Dharwar Craton, India: 2.52 Ga U–Pb ages of hydrothermal monazite and xenotime in gold deposits; *Mineral. Deposita* **46** 273–288.

Sarvothaman H 2001 Archean high-Mg granitoids of mantle origin in the Eastern Dharwar Craton of Andhra Pradesh; *J. Geol. Soc. India* **58** 261–268.

Saxena P R and Sudarshan V 1997 Occurrence of molybdenite in the granites of Pirancheru near Hyderabad, Andhra Pradesh; *J. Geol. Soc. India* **50** 347–348.

Shand S J 1943 *The Eruptive Rocks*; 2nd edn (New York: John Wiley).

Shirey S B and Hanson G N 1986 Mantle heterogeneity and crustal recycling in Archean granite-greenstone belts: Evidence from Nd isotopes and trace elements in the Rainy Lake area, Superior Province, Ontario, Canada; *Geochim. Cosmochim. Acta* **50** 2631–2651.

Shukla S and Ram Mohan M 2019 Magma mixing in Neoarchean granite from Nalgonda region, Eastern Dharwar Craton, India: Morphological, mineralogical and geochemical evidences; *J. Earth Syst. Sci.* **128** 71.

Singh A P, Kumar V V and Mishra D C 2004 Subsurface geometry of Hyderabad granite pluton from gravity and magnetic anomalies and its role in the seismicity around Hyderabad; *Curr. Sci.* **86** 580–586.

Singh T D, Manikyamba C, Lakshminarayana G and Subramanyam K S V 2017 Geochemical signatures of adoni porphyritic granitoids, Eastern Dharwar Craton, India: Implication for partial melting of lower continental crust; *J. Appl. Geochem.* **19** 183.

Singh P K, Verma S K, Singh V K, Moreno J A, Oliveira E P and Mehta P 2019 Geochemistry and petrogenesis of sanukitoids and high-K anatectic granites from the Bundelkhand Craton, India: Implications for late-Archean crustal evolution; *J. Asian Earth Sci.* **174** 263–282.

Sitaramayya S 1971 The pyroxene-bearing granodiorites and granites of Hyderabad area (The Osmania granite); *Quat. J. Geol. Min. Metal. Soc. India* **43** 117–129.

Smithies R H and Witt W K 1997 Distinct basement terranes identified from granite geochemistry in late Archaean granite-greenstones, Yilgarn Craton, Western Australia; *Precamb. Res.* **83** 185–201.

Smithies R H and Champion D C 2000 The Archaean high-Mg diorite suite: Links to tonalite–trondhjemite–granodiorite magmatism and implications for early Archaean crustal growth; *J. Petrol.* **41** 1653–1671.

Smithies R H, Champion D C and Van Kranendonk M J 2009 Formation of Paleoarchean continental crust through intracrustal melting of enriched basalt; *Earth Planet. Sci. Lett.* **281** 298–306.

Spitz G and Darling R 1978 Major and minor element lithogeochemical anomalies surrounding the Louvem copper deposit, Val d'Or, Quebec; *Can. J. Earth Sci.* **15** 1161–1169.

Subba Rao M V, Rama Rao P and Divakara Rao V 1998 The advent of the Proterozoic—a trigger for extensive intracrustal processes in the south Indian Shield? *Gondwana Res.* **1** 275–283.

Sun S S and McDonough W F 1989 Chemical and isotopic systematics of oceanic basalts: Implications for mantle composition and processes; *Geol. Soc. London Spec. Publ.* **42** 313–345.

Swami Nath J and Ramakrishnan M (eds) 1981 Early Precambrian supracrustals of southern Karnataka; *Geol. Surv. India Memoir* **112,** 352.

Sylvester P J 1994 Archean granite plutons; In: *Archean Crustal Evolution* (ed.) Condie K C, Amsterdam, pp. 261–314.

Szilas K and Garde A 2013 Mesoarchaean aluminous rocks at Storø, southern West Greenland: new age data and evidence of premetamorphic seafloor weathering of basalts; *Chem. Geol.* **354** 124–138.

Taylor S R and McLennan S M 1985 The geochemical evolution of the continental crust; *Rev. Geophys.* **33** 241–265.

Thompson A B and Connolly J A 1995 Melting of the continental crust: Some thermal and petrological constraints on anatexis in continental collision zones and other tectonic settings; *J. Geophys. Res. Solid Earth* **100** 15,565–15,579.

Turner S, Sandiford M and Foden J 1992 Some geodynamic and compositional constraints on 'post orogenic' magmatism; *Geology* **20** 931–934.

Van Kranendonk M J, Hugh Smithies R, Hickman A H and Champion D C 2007 Secular tectonic evolution of Archean continental crust: Interplay between horizontal and vertical processes in the formation of the Pilbara Craton, Australia; *Terra Nova* **19** 1–38.

Verma S P and Díaz-González L 2012 Application of the discordant outlier detection and separation system in the geosciences; *Int. Geol. Rev.* **54** 593–614.

Verma S P, Pandarinath K, Verma S K and Agrawal S 2013 Fifteen new discriminant-function-based multi-dimensional robust diagrams for acid rocks and their application to Precambrian rocks; *Lithos* **168** 113–123.

Ward C D, McArthur J M and Walsh J N 1992 Rare earth element behaviour during evolution and alteration of the Dartmoor Granite, SW England; *J. Petrol.* **33** 785–815.

Whalen J B, Currie K L and Chappell B W 1987 A-type granites: geochemical characteristics, discrimination and petrogenesis; *Contrib. Mineral. Petrol.* **95** 407–419.

Whalen J B, Percival J A, McNicoll V J and Longstaffe F J 2004 Geochemical and isotopic (Nd–O) evidence bearing on the origin of late- to post-orogenic high-K granitoid rocks in the western Superior Province: Implications for late-Archaean tectonomagmatic processes; *Precamb. Res.* **132** 303–326.

Winchester J A and Floyd P A1977 Geochemical differentiation of different magma series and their differentiation products using immobile elements; *Chem. Geol.* **20** 325–343.

Zhai M 2014 Multi-stage crustal growth and cratonization of the North China Craton; *Geosci. Frontiers* **5** 457–469.

Corresponding editor: Rajneesh Bhutani